Chapter 2

Synthesis and mesomorphic properties of

(i) 4-((4-Cyanophenoxy)carbonyl)phenyl-4′-(4-*n*-alkoxybenzoyloxy)-biphenyl-3-carboxylates, (compounds 2.A.1 to 2.A.7)

(ii) 4-Cyanophenyl-3′-(4-(4-*n*-alkoxybenzoyloxy)benzoyloxy)biphenyl-4-carboxylates, (compounds 2.B.1 to 2.B.9)

(iii) 4-Cyano-3-fluorophenyl-3′-(4-(4-*n*-alkoxybenzoyloxy)-benzoyloxy)biphenyl-4-carboxylates, (compounds 2.B.10 to 2.B.12)

2.1: Introduction

During the past several years, a few thousand compounds composed of achiral bent-core (BC) molecules have been synthesized and the mesophases exhibited by them investigated. This is due to the discovery [1] of electro-optical switching in the mesophase of such a BC compound. In addition, the various results obtained from these are quite fascinating, exciting, intriguing and one of the most striking features is the observation of polar switching in such compounds even though the constituent molecules are achiral [2-5]. Apart from well established banana mesophases B_1-B_8, conventional calamitic phases such as nematic, smectic A and smectic C phases have also been observed in BC compounds. If the molecules of such a compound organize themselves orthogonally with respect to the layer plane then a polar smectic A phase can be realized and these are more promising applicants for new technologies.

Theoretical prediction of McMillan (biaxial smectic A) phase

The existence of a biaxial smectic A phase (SmA_b) was theoretically predicted [6] by de Gennes more than thirtyfive years ago. This phase is also called the smectic C_M phase, where M refers to McMillan. Brand, Cladis and Pleiner [7] suggested that C_M phase (biaxial smectic phase) could be realized in board-like molecules. They predicted defects and the properties of smectic C_M phase based on symmetry arguments. In smectic A, a layered state, the layer normal is a unit vector **p** and is indistinguishable from –**p**. In the plane of its layers the director, **n** is parallel to layer normal, **p**. In the SmA phase the director is constant everywhere and shows no defect. The uniaxial nematic and smectic A liquid crystals have $D_{\infty h}$ symmetry.

In classical smectic C phase, the director **n** is at a constant tilt angle to the layer normal, **p** at constant temperature. The projection of director on layer plane is denoted by vector **c**. The smectic C phase ground state is invariant unless the two symmetry operations **p** to –**p** and **c** to –**c** are performed simultaneously. Smectic C phase is biaxial and has C_{2h} point symmetry. In SmC, **c** is not equivalent to **–c** and only ±1 strength defects (2π rotations) are possible and no ±½ defects (π rotations) are allowed by its symmetry.

In the biaxial smectic (C_M) phase, tilt is absent, **n** is parallel to **p**. The in-plane preferred direction is characterized by director **m** and is perpendicular to **p**. The ground state remains unchanged during a change over from **p** to –**p** and **m** to –**m**. In contrast, smectic C_M phase can show true ±½ disclinations in addition to ±1 defects and this is because smectic C_M phase has D_{2h} symmetry. A pictorial representation of molecules in smectic A, C and C_M phases are shown in figures **2.1.a, 2.1.b** and **2.1.c** respectively.

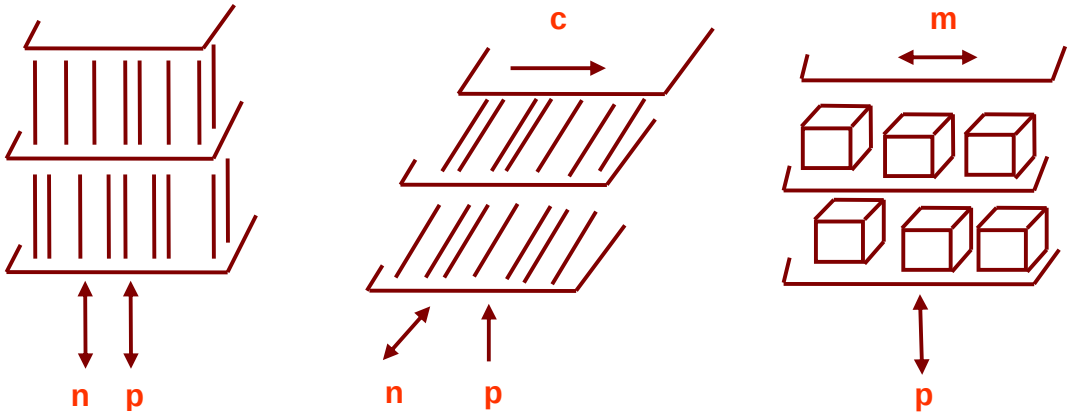

Figure 2.1: Schematic representation of molecular director (n), layer normal (p), projection of molecular director (c), in-plane director (m), for the (a) SmA, (b) SmC and (c) C_M mesophases (after Brand *et al.* [7]).

The important feature of smectic phases is the occurrence of focal-conic or fan-shaped texture where they conserve microscopic layer spacing when the layers are curved. Since layer curvature energy is small, the focal-conic textures are easily observed under a polarizing optical microscope without any special treatment during sample preparation. When a transition takes place from SmA to SmC phase, because of the mismatch in the layer spacing the focal-conics become broken focal-conics. However, while going from SmA to SmA_b phase, no broken focal-conics are observed because of its **m** = **-m** symmetry and there is no mismatch in the layer

spacings. Thus, these qualitative microscopic observations would help to distinguish the biaxial smectic A phase from the classical SmC phase.

Bent-core molecules are biaxial in nature due to their intrinsic shape. These molecules can arrange either orthogonally (SmAP) or can tilt (SmCP) in the layers with respect to the layer normal in order to exhibit a polar phase and a pictorial representation of these are shown in figure **2.2.**

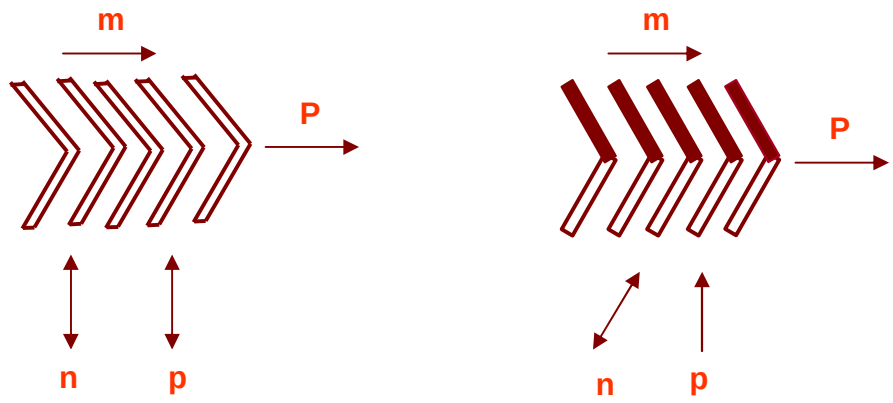

SmAP (C_{2V} symmetry) SmCP (C_2 symmetry)

(a) **(b)**

Figure 2.2: Schematic representation of bent-core molecules in (a) biaxial smectic A phase, side view; (b) biaxial smectic C phase side view (after Amaranatha Reddy and Sadashiva [15]).

Experimental observations of biaxial smectic A phase

The first experimental evidence for the biaxial smectic A phase was provided by Leube and Finkelmann [8] in a binary mixture of a liquid crystalline polymer and a monomeric material. Later, Pratibha *et al.* provided the first experimental evidence [9] for the existence of a biaxial smectic A phase in low molecular mass compounds, although in a mixture of BC compounds and rod-shaped compounds. At a concentration of 4-13 mol% of BC molecules a new phase is observed with two- and four-brush defects on lowering the temperature from

bilayer uniaxial smectic A phase. The schlieren texture with two-brush defects observed is due to the orientational transition of BC molecules in layers, with the director being orthogonal to the rod-shaped molecules which gives rise to orthogonal biaxial phase. Hence, this phase is designated as bilayer biaxial smectic A (SmA_{2b}) phase. Subsequently, Hegmann *et al.* [10] reported the first example of a single layer biaxial smectic A phase in a binary mixture of a metallomesogen and 2, 4, 7-trinitrofluorenone.

In 1998, Semmler *et al.* [11] investigated a symmetric, low molecular mass liquid crystal composed of bent-shape molecules derived from oxadiazole central unit. They claimed to have observed the biaxial smectic A phase, although unambiguous proof has not been provided. The first biaxial smectic A phase showing antiferroelectric behaviour in achiral bent-core compound derived from 4-cyanoresorcinol was reported by Eremin *et al.* [12] in 2001 with sufficient experimental proof.

We have been actively involved in designing and synthesizing new materials for obtaining the biaxial smectic A phase in BC compounds for a few years. For example, we have reported [13-16] the synthesis of several compounds composed of strongly polar unsymmetrically substituted BC molecules which exhibit the partial bilayer biaxial smectic A phase. All these compounds derived from 3-hydroxybenzoic acid contain a highly polar terminal cyano group which overlap in an antiparallel orientation. These studies, have revealed transitions from a partial bilayer uniaxial smectic (SmA_d) phase to a partial bilayer polar biaxial smectic A (SmA_dP_A) phase with antiferroelectric properties and a nematic phase to a SmA_dP_A phase. These represent the first observations of such phase transitions.

A few years ago, Mieczkowski *et al.* reported the occurrence of a higher temperature uniaxial ferroelectric phase [17] and a lower temperature B_{1RT} phase in asymmetric bent-shaped molecules derived from 2-methylresorcinol. The theoretical and experimental evidence for the occurrence of such phases was provided by Pociecha [18] and Shimbo *et al.* [19] for the higher temperature smectic phase which has a non-tilted, optically uniaxial and polarly ordered structure with random direction of the layer polarization occurring in asymmetric bent-shaped molecules. This was called the $SmAP_R$ phase and has been reported to be important for technological applications particularly for fast switching display devices [20]. Recently some

new asymmetric compounds exhibiting this phase have been reported [21]. The first symmetric compounds composed of bent-core molecules exhibiting $SmAP_R$ and $SmAP_A$ phases have been reported [22] by Gomola *et al.* Later Guo *et al.* [23] found experimentally that the phase transition occurs from a locally polar ordered phase to a macroscopically antiferroelectrically ordered phase using X-ray diffraction, electro-optical, second harmonic generation and dielectric studies.

The unique phase sequence of SmA-$SmAP_R$-$SmAP_A$ was reported [24] by Keith *et al.* in the bent-core compounds derived from 4-cyanoresorcinol. The molecular arrangement of orthogonal phases of $SmAP_A$ and $SmAP_R$ have been shown in figure **2.3.**

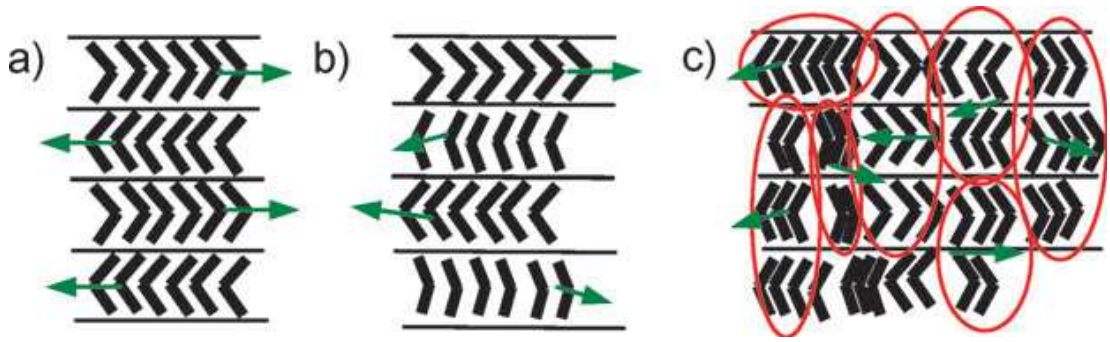

Figure 2.3: Models of molecular arrangements (green arrows = polar direction, skewed arrows point out of or into the projection plane): (a) $SmAP_A$; (b,c) $SmAP_R$; (b) randomization of polar direction between the layers, (c) randomization of polar direction within the layers (ferroelectric clusters) (after Keith *et al.* [24]).

Very recently, Reddy *et al.* reported [25] the first example of SmA-$SmAP_F$ phase transition in a bent-core compound, containing polar cyano group in one end where as the other end is a tail with carbosilane group. This was found to be the first fluid smectic ferroelectric phase with orthorhombic symmetry and this is the highest-symmetry ferroelectric material found to date. The parallel alignment of the molecular dipoles in the adjacent layers are stabilized by terminal silane group that leads to three-dimensional orthorhombic ferroelectric structure and this was determined by electro-optical studies.

However, the occurrence of orthogonal smectic mesophases is very rare in BC compounds but has been achieved by special molecular design. In this chapter, the synthesis and characterization of unsymmetrical compounds containing a strongly polar cyano group at one terminal position while the other end is substituted by an *n*-alkoxy chain are described. In one of the series, the effect of a fluoro substituent *ortho* to the terminal cyano group is also examined. The unsymmetrical compounds described here have the general molecular structures **2.1** and **2.2** shown below.

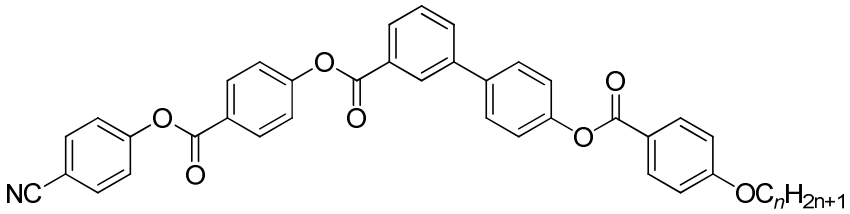

Structure 2.1

n = 12, 13, 14, 15, 16, 18, 20 Series **2.A**

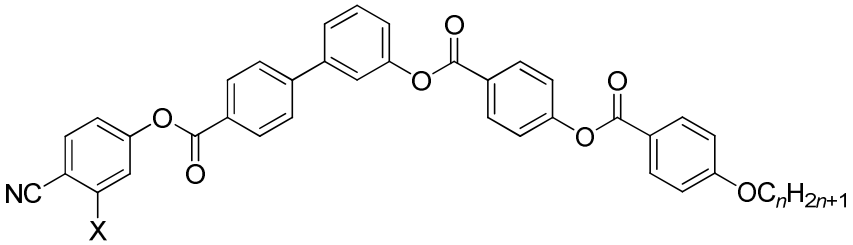

Structure 2.2

X = H *n* = 10, 11, 12, 13, 14, 15, 16, 18, 20 Series **2.B**

X = F *n* = 16, 18, 20 Series **2.B**

2.2: Synthesis

Two new homologous series of novel five-ring unsymmetrical bent-core compounds containing 3,4-disubstituted biphenyl unit have been synthesized. Compounds of series **2.A** were synthesized by following a route shown in scheme **2.2**, and compounds of series **2.B** were prepared following a pathway shown in scheme **2.5.**

Methyl 3-(4-hydroxyphenyl)benzoate, methyl 3-hydroxybiphenyl-4-carboxylate and benzyl 4-hydroxybenzoate were obtained from Aldrich Chemicals Pvt. Ltd. and used without further purification. The other materials 4-cyanophenol and 2-fluoro-4-cyanophenol were also obtained from commercial sources. 4-Benzyloxybiphenyl-3-carboxylic acid, **2.c** was prepared by benzylation of methyl 3-(4-hydroxyphenyl)benzoate using benzyl chloride and anhydrous potassium carbonate in anhydrous butan-2-one followed by hydrolysis of the ester using aq. KOH and ethanol and the synthetic route used is outlined in scheme **2.1.** Similarly, 3-benzyloxybiphenyl-4-carboxylic acid, **2.j** was also prepared as shown in scheme **2.3.** 4-*n*-Alkoxybenzoic acid was esterified with benzyl 4-hydroxybenzoate using *N*,*N*′-dicyclohexylcarbodiimide (DCC) and a catalytic amount of 4-(*N*,*N*-dimethylamino)pyridine (DMAP) in dichloromethane followed by hydrogenolysis using 5% Pd-C in an hydrogen atmosphere which provided the two-ring acids, **2.m** and the synthetic route used is given in

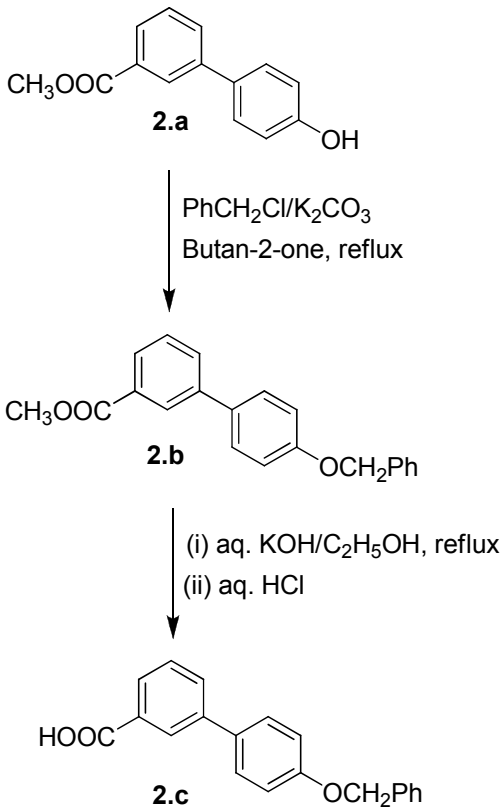

Scheme 2.1: Synthetic route employed for preparation of 4-benzyloxybiphenyl-3-carboxylic acid, 2.c.

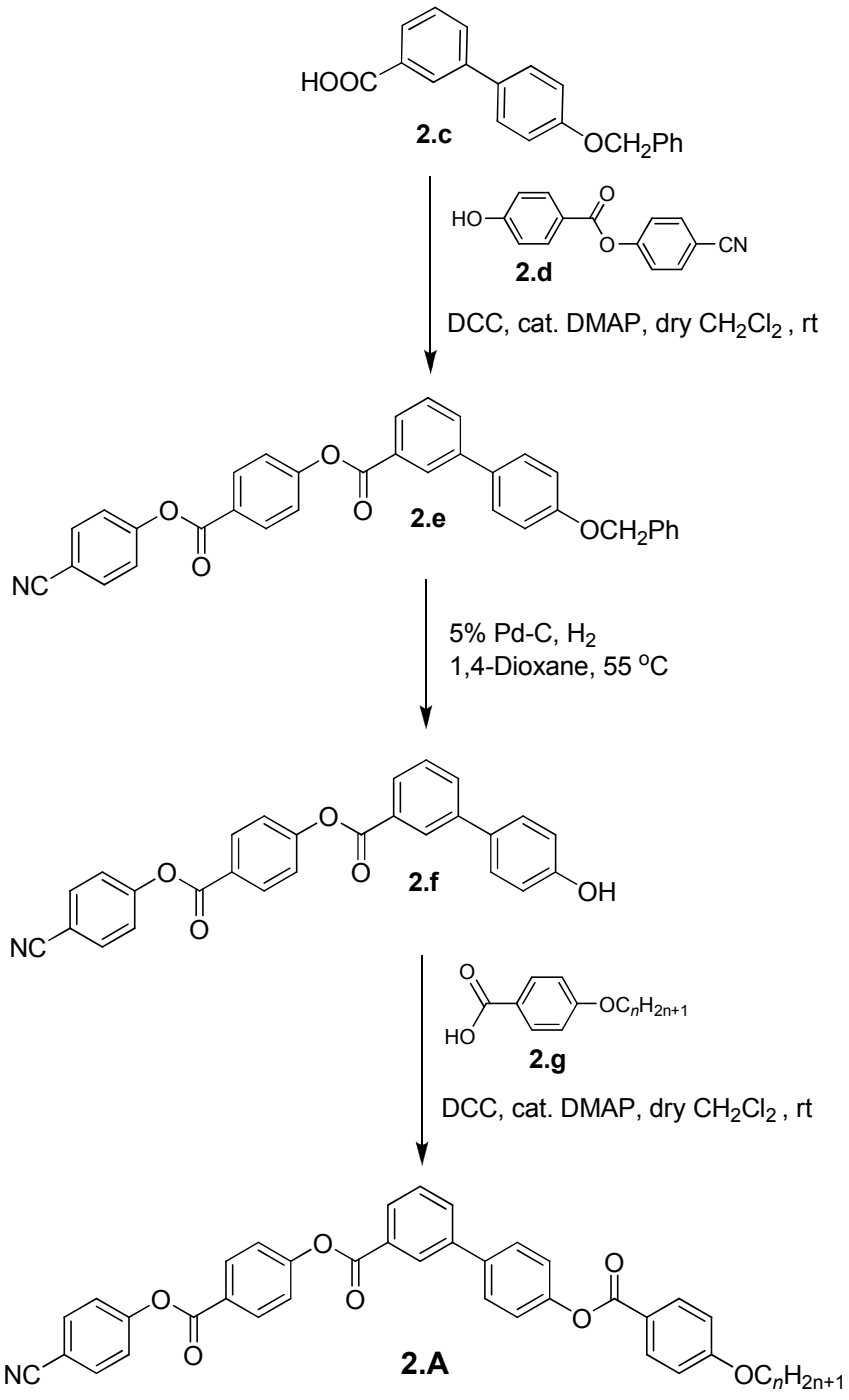

Scheme 2.2: Synthetic pathway followed for preparation of BC compounds of series 2.A.

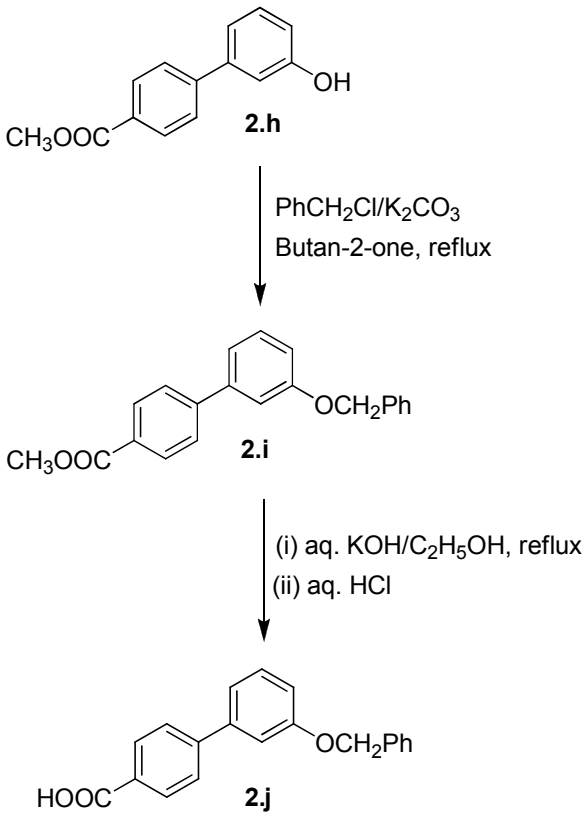

Scheme 2.3: Synthetic route followed for preparation of 3-benzyloxybiphenyl-4-carboxylic acid, 2.j.

scheme **2.4.** 4-Cyanophenyl-4-hydroxybenzoate, **2.d** [14] was prepared following a procedure described in the literature.

2.3: Results and discussion

2.3.1: Mesomorphic properties

The transition temperatures and the associated enthalpy values obtained for these novel five-ring bent-core compounds belonging to series **2.A** and **2.B** are summarized in tables **2.1** and **2.2** respectively. All compounds synthesized and investigated are mesomorphic. As can be seen in table **2.1**, compounds **2.A.1** to **2.A.5** show only one mesophase and compound **2.A.1** is

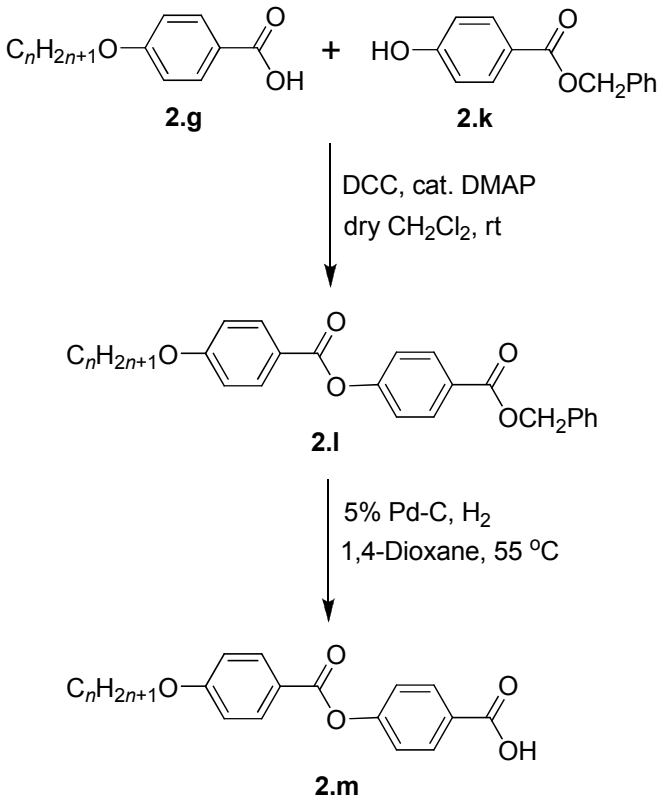

Scheme 2.4: Synthetic route used for preparation of two-ring acids 2.m.

monotropic and compounds **2.A.2** to **2.A.5** are enantiotropic. When a thin film of a sample of compound **2.A.3** was sandwiched between two glass plates and cooled slowly from the isotropic phase, batonnets appear which coalesce to form a schlieren texture with two- and four-brush defects. In addition, striped pattern could also be seen in some regions and the optical texture obtained is shown in figure **2.4.** This striped pattern [14, 15] is a typical texture observed for biaxial smectic A phase. On shearing the sample there is no dark region observed indicating the mesophase is biaxial and thus, the possibility of this phase being uniaxial SmA can be ruled out. The two- and four-brush defects can be seen in the following cases. (i) SmC_a phase in which molecules of adjacent layers have anticlinic arrangement or (ii) A biaxial smectic A phase in which the two orthogonal directors are in the plane of smectic layers. X-Ray diffraction measurements of a powder sample was carried out on the mesophase for the same sample. Two sharp reflections in the small angle region at $d_1 = 50.39$ Å and $d_2 = 25.2$ Å which are in the ratio

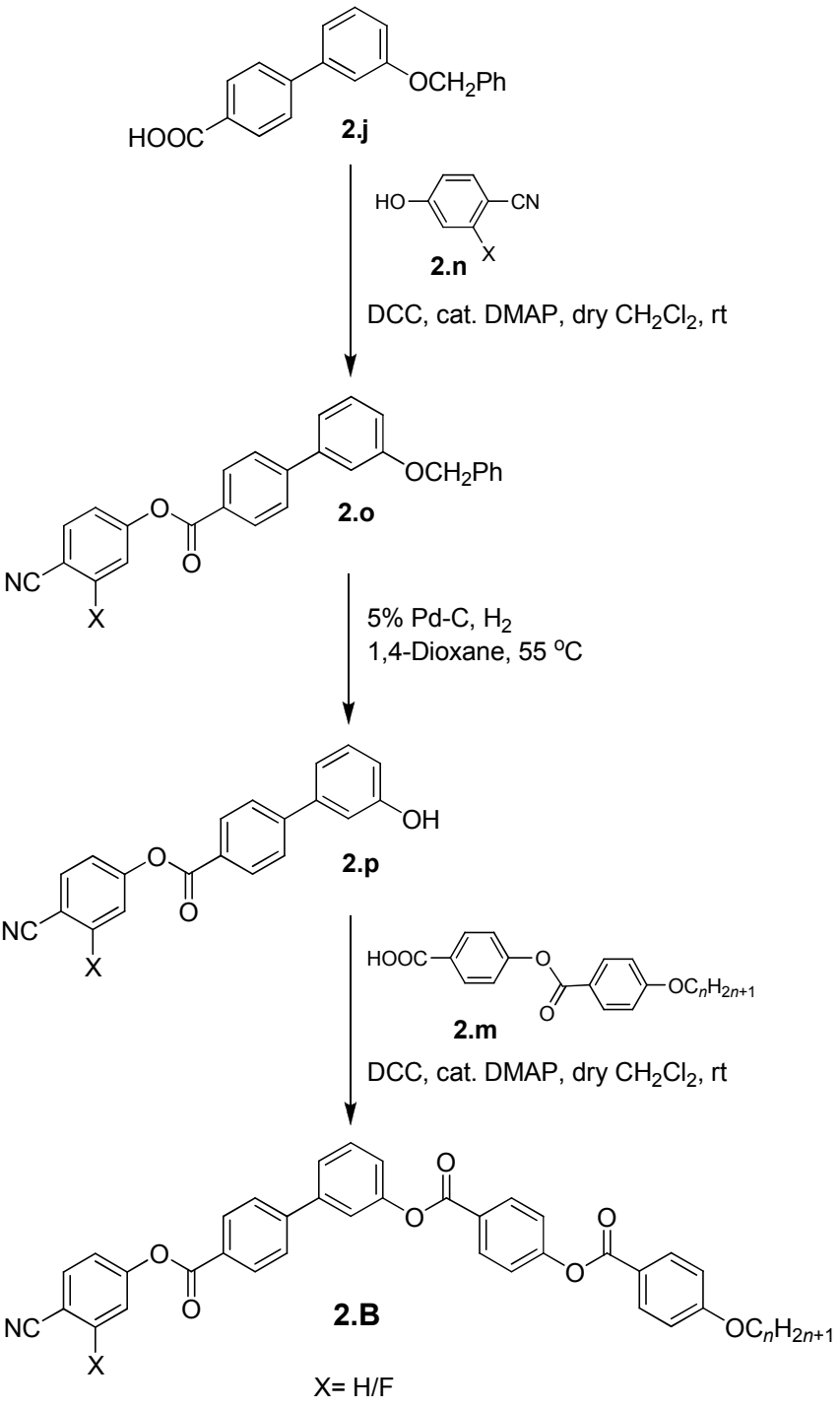

Scheme 2.5: Synthetic pathway employed for preparation of BC compounds of series 2.B.

Table 2.1: Transition temperatures (°C) and the associated enthalpy values (kJ mol^{-1}) (in italics) for compounds of series 2.A[a]

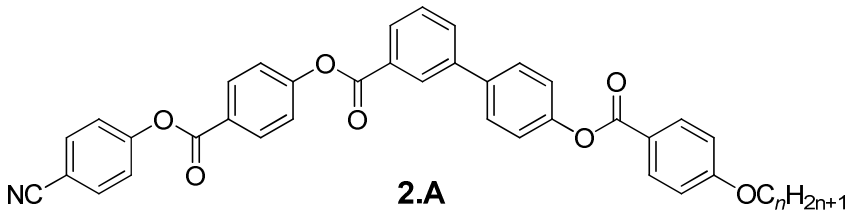

2.A

Compound	*n*	Cr		SmA_dP_A		SmA_dP_R		I
2.A.1	12	•	147.0 *163.0*	(•	131.0) *9.5*	-		•
2.A.2	13	•	134.5 *112.0*	•	136.0 *10.0*	-		•
2.A.3	14	•	135.5 *122.5*	•	140.0 *10.5*	-		•
2.A.4	15	•	134.5 *117.0*	•	143.0 *10.5*	-		•
2.A.5	16	•	135.0 *114.5*	•	146.0 *11.0*	-		•
2.A.6	18	•	134.5 *101.0*	•	148.0 *0.06*	•	150.0 *10.0*	•
2.A.7	20	•	134.5 *113.5*	•	149.0 *0.09*	•	153.0 *9.5*	•

[a]Abbreviations: Cr: crystalline phase; SmA_dP_A: partial bilayer biaxial antiferroelectric smectic A phase; SmA_dP_R: partial bilayer polar uniaxial smectic A phase; I: isotropic phase; ( ): phase is monotropic; •: phase exists; - : phase does not exist.

1 : 1/2 were obtained which suggest that the mesophase is a smectic phase. In addition, a diffuse wide-angle peak with a maximum at 4.7 Å was obtained indicating a liquid-like in-plane order. It can be seen that the first order layer spacing d, is significantly larger than the calculated molecular length L, but less than 2L indicating a partial bilayer structure. Based on XRD measurements and electro-optical switching studies (described later) the mesophase of compound **2.A.3** is designated as a partial bilayer smectic A phase which is polar and

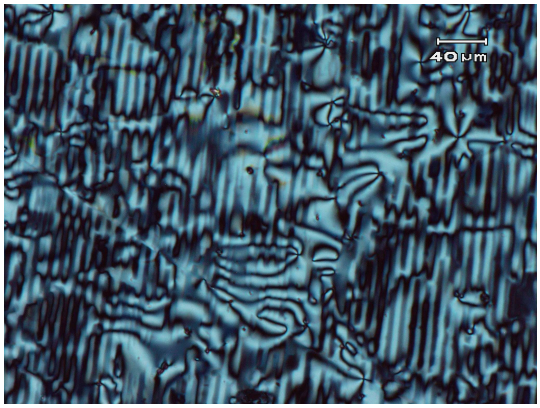

Figure 2.4: Optical texture obtained for the SmA_dP_A phase of compound 2.A.3 at T = 135 °C.

antiferroelectric (SmA_dP_A) phase. The other lower homologues viz., **2.A.1, 2.A.2, 2.A.4** and **2.A.5** exhibit optical textures and electro-optical switching behaviour similar to that shown by compound **2.A.3.** Hence, the mesophase exhibited by all of them are of the same type.

Interestingly, compounds **2.A.6** and **2.A.7** show an additional mesophase at higher temperatures. When a sample of compound **2.A.7** was cooled slowly from the isotropic phase in a cell treated for homogeneous alignment, a focal-conic texture that is typically seen for a smectic A phase was observed and on lowering the temperature further, transition bars were seen to grow across the focal-conics as shown in figure **2.5.a** and **2.5.b** respectively. When a sample of this compound was cooled slowly from the isotropic phase in a cell treated for homeotropic alignment, a dark texture was obtained as shown in figure **2.5.c** which indicates uniaxiality of the phase. On cooling further to the lower temperature phase, again a schlieren texture with two- and four-brush defects as shown in figure **2.5.d** was obtained. This is a clear signature for the biaxial smectic A phase as reported [14, 15] earlier. A DSC thermogram obtained for compound **2.A.7** is given in figure **2.6** which clearly shows the phase transitions. XRD measurements and electro-optical studies (described later) confirmed that the higher temperature phase is a partial bilayer polar randomized uniaxial smectic A (SmA_dP_R) phase and lower temperature phase is

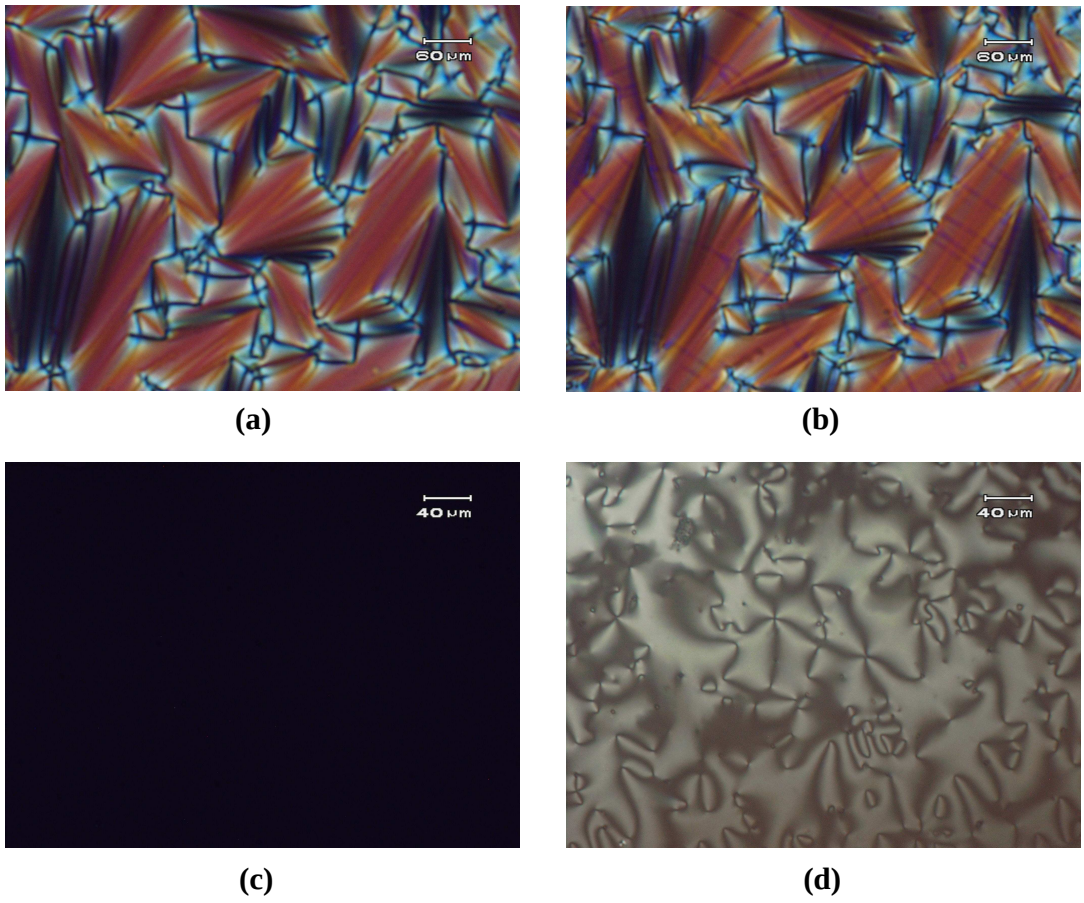

Figure 2.5: (a) and (b): Optical textures of the mesophases exhibited by compound 2.A.7 in a cell treated for planar alignment at T = 150 °C and T = 145 °C respectively; (c) and (d): Textures of the same mesophases in a cell treated for homeotropic alignment (same temperatures).

SmA_dP_A. A plot of the transition temperature as a function of the number of carbon atoms in the terminal chain for this series of compounds is shown in figure **2.7.** One can clearly see a smooth ascending curve for the mesophase to isotropic/mesophase transition points. Compound **2.A.7** shows a thermal range of 4 °C for SmA_dP_R and 14.5 °C for SmA_dP_A phases.

Compounds belonging to series **2.B** were obtained from 3-benzyloxybiphenyl-4-carboxylic acid which is an isomer of central unit of series **2.A.** As can be seen in table **2.2,** all

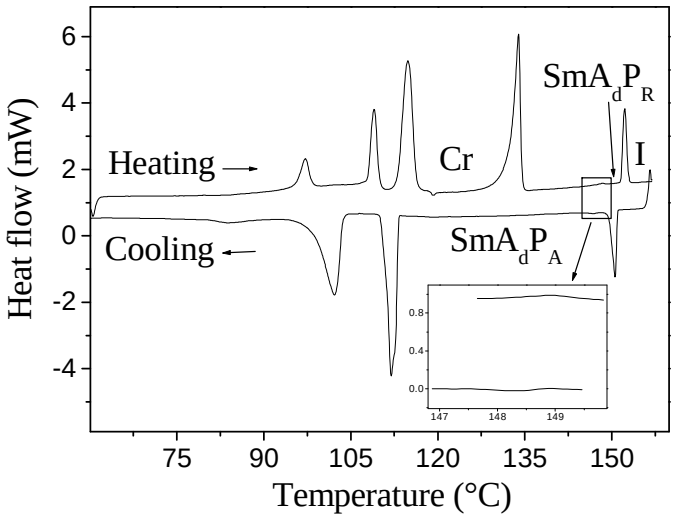

Figure 2.6: A DSC thermogram obtained for compound 2.A.7 showing phase transitions; rate 5 °C min^{-1}; Expanded region of transition from a polar uniaxial SmA to a polar biaxial SmA phase is shown in inset.

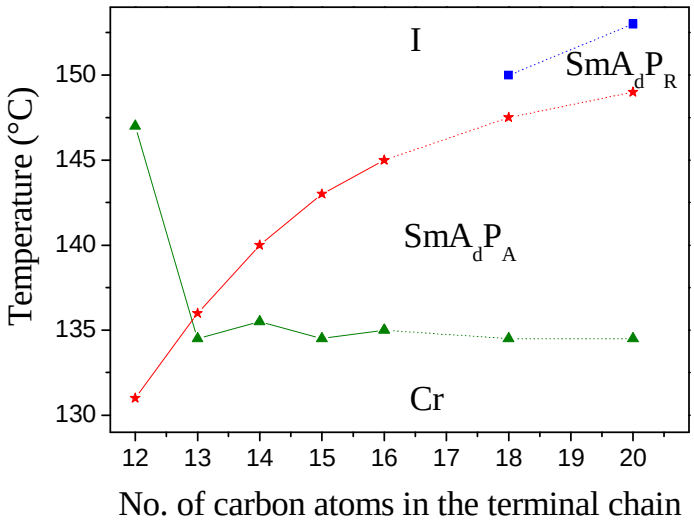

Figure 2.7: Plot of transition temperature versus number of carbon atoms in the terminal *n*-alkoxy chain for the homologues of series 2.A.

Table 2.2: Transition temperatures (°C) and the associated enthalpy values (kJ mol^{-1}) (in italics) for compounds of series 2.B[a]

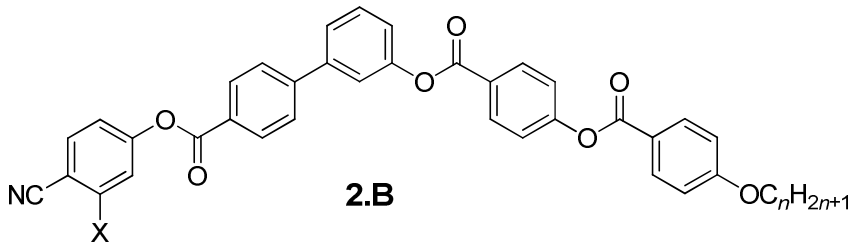

2.B

Compound	*n*	X	Cr		SmA_{db}		SmA_d		I
2.B.1	10	H	•	115.5 *145.5*	(•	95.5) *6.5*	-		•
2.B.2	11	H	•	104.0 *116.0*	(•	101.5) *7.5*	-		•
2.B.3	12	H	•	118.0 *217.5**	(•	107.5) *9.5*	-		•
2.B.4	13	H	•	122.0 *151.5*	(•	113.0) *9.5*	-		•
2.B.5	14	H	•	115.5 *108.0**	•	117.5 *9.5*	-		•
2.B.6	15	H	•	116.5 *109.0**	•	121.5 *10.0*	-		•
2.B.7	16	H	•	115.0 *101.0**	•	125.0 *10.5*	-		•
2.B.8	18	H	•	116.0 *113.5**	•	130.5 *10.5*	-		•
2.B.9	20	H	•	116.0 *99.0*	•	133.0 *10.0*	-		•
2.B.10	16	F	•	114.5 *120.5*	(•	112.5) *7.5*	-		•
2.B.11	18	F	•	117.0 *123.5*	•	118.5 *0.06*	•	120.0 6.*5*	•
2.B.12	20	F	•	118.5 *124.0*	•	120.0 *0.2*	•	125.0 *5.5*	•

[a]See **Table 2.1**: *has crystal-crystal transition; enthalpy denoted is the sum of all such transitions; SmA_{db}: partial bilayer biaxial smectic A phase; SmA_d: partial bilayer uniaxial smectic A phase.

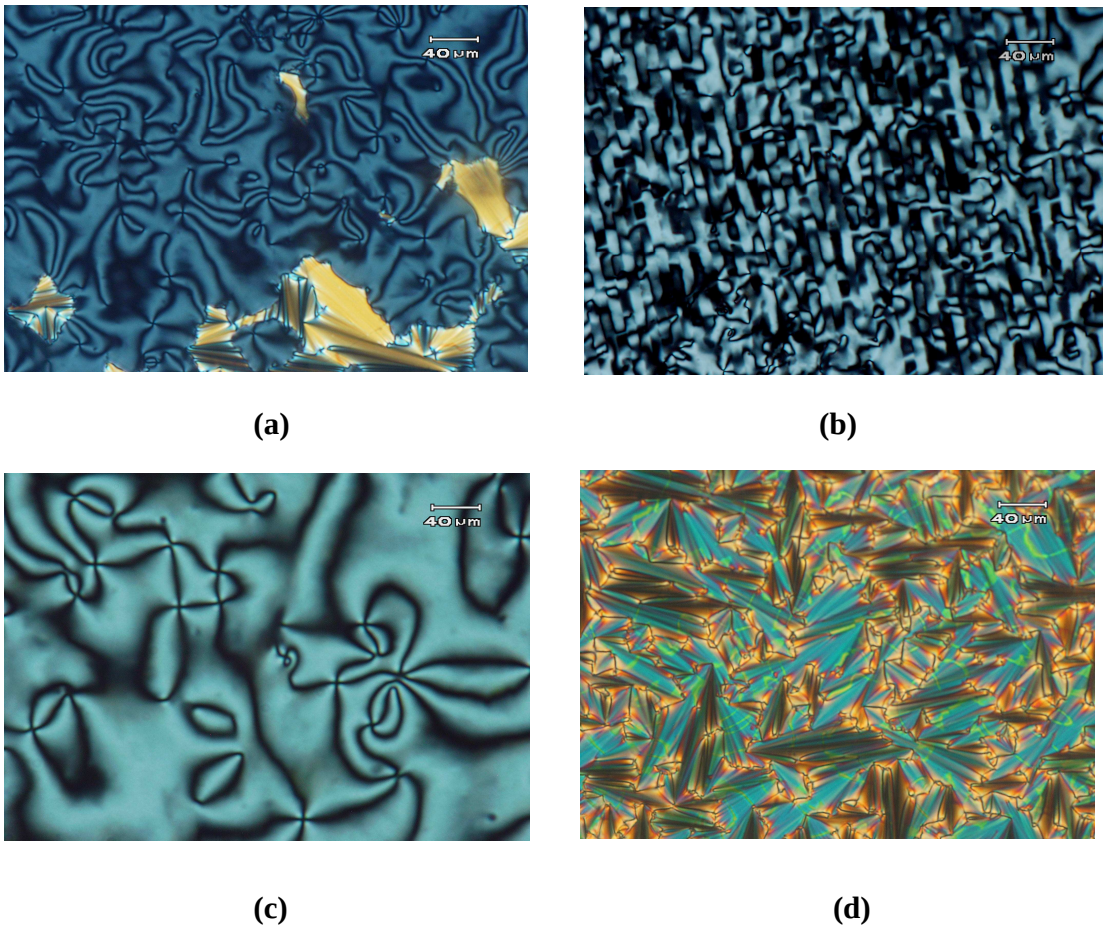

Figure 2.8: Photomicrographs of the optical textures exhibited by compound 2.B.8 between two ordinary glass plates. (a) Schlieren texture with focal conics at T = 125.6 °C; (b) striped pattern of SmA_{db} phase at T = 125 °C; (c) schlieren texture with two- and four-brush defects at T = 125 °C in a cell treated for homeotropic alignment; (d) fan-shaped texture with arcs across the fans at T = 122.8 °C of the same sample in a cell treated for homogeneous alignment.

the parent compounds (without any lateral substituent) exhibit only one mesophase. While compounds **2.B.1** to **2.B.4** show a metastable mesophase, compounds **2.B.5** to **2.B.9** are enantiotropic in nature. When a sample of compound **2.B.8** was sandwiched between two untreated glass plates and cooled slowly from the isotropic state, a schlieren texture with predominantly two- and four-brush defects along with focal-conics was obtained as shown in

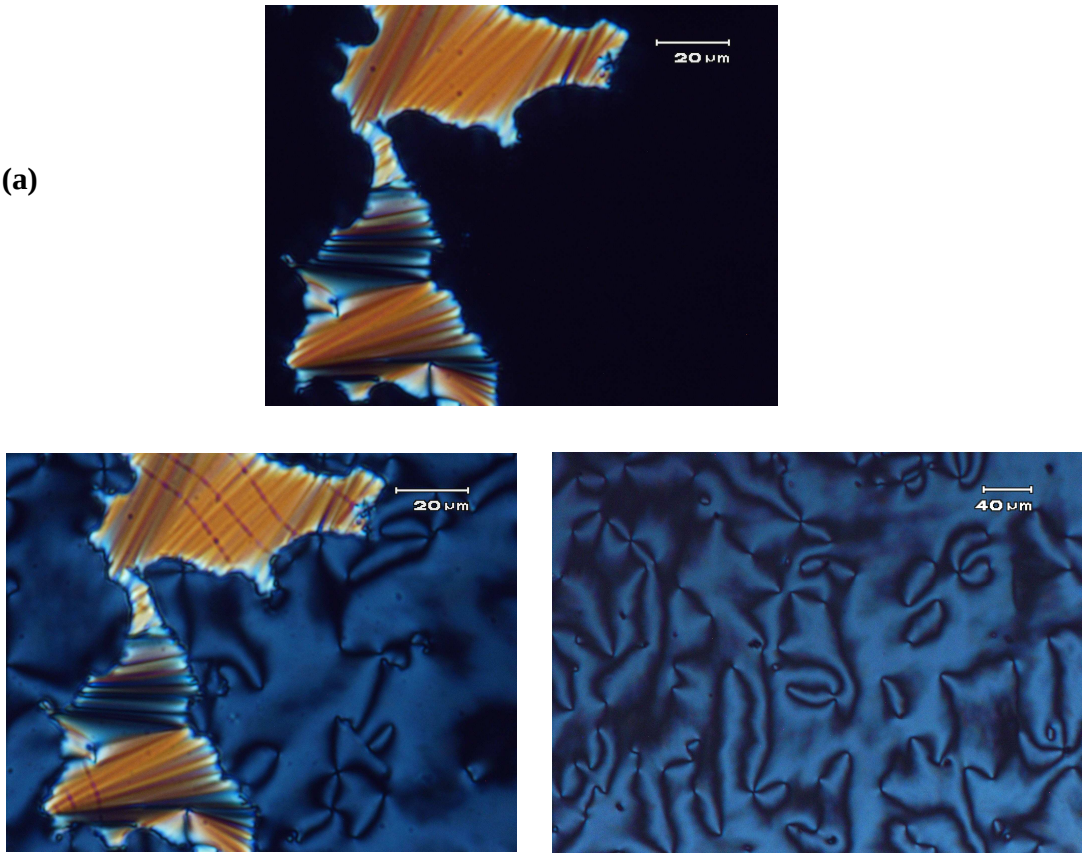

Figure 2.9: Photomicrographs of the textures exhibited by compound 2.B.11. (a) SmA_d phase at T = 119 °C; (b) same region as in (a) at T = 117 °C showing appearance of the biaxial smectic (SmA_{db}) phase. Note dark lines appearing across the fans. (c) Different region of the same cell showing two- and four-brush defects in the schlieren texture.

figure **2.8.a.** After shearing the sample, it was heated to the isotropic phase and cooled again to the mesophase. A striped pattern as shown in figure **2.8.b** was obtained. This behaviour is again typically seen for a orthogonal biaxial smectic phase. A confirmation of this was obtained when a sample of this compound was observed in cells treated for homeotropic and homogeneous

(a)

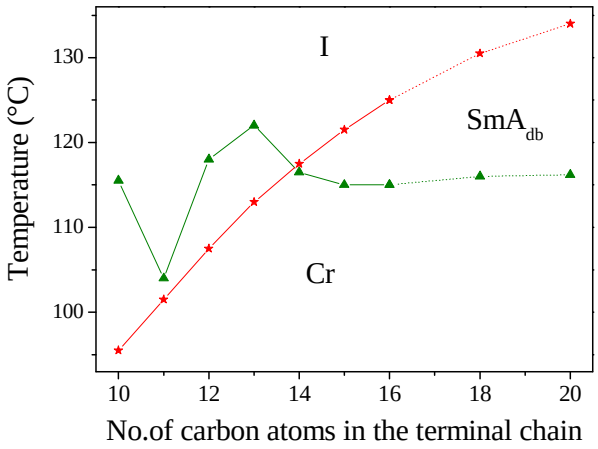

(b)

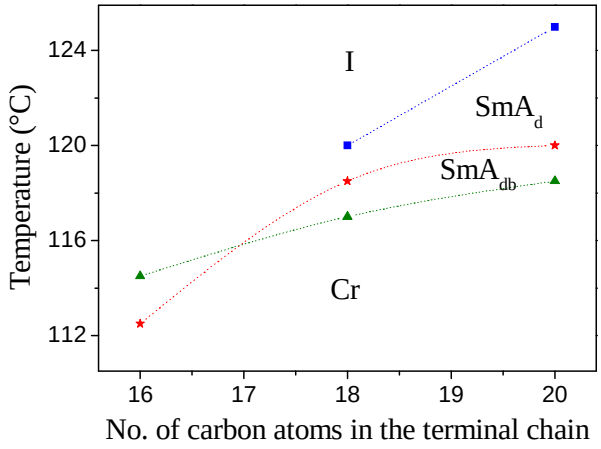

Figure 2.10: (a) Plot of transition temperature as a function of the number of carbon atoms in the terminal *n*-alkoxy chain for the homologues of parent compounds (2.B.1 to 2.B.9) of series 2.B. (b) Similar plot for fluorine substituted compounds (2.B.10 to 2.B.12) of series 2.B.

alignments. A schlieren texture with two- and four-brush defects for the homeotropic alignment and a focal-conic texture with arcs across the fans for the homogeneous alignment were obtained as shown in figures **2.8.c** and **2.8.d** respectively. As described later this mesophase has been designated as a partial bilayer biaxial smectic A (SmA_{db}) phase.

In order to examine the effect of a fluorine substituent *ortho* to the terminal cyano group, three such compounds **2.B.10** to **2.B.12** were prepared. Interestingly, the melting points were not affected much, but the clearing points decreased. Surprisingly an additional phase was induced for longer *n*-alkoxy chain and this phase has been identified as a partial bilayer uniaxial smectic A phase (SmA_d). The transition temperatures and associated enthalpy values of these fluorine substituted compounds are also summarized in table **2.2** along with parent compounds and for comparison. Similar optical textures were seen for these compounds as well, for e.g. by slow cooling of the isotropic phase of **2.B.11** in a cell treated for homeotropic alignment. These textures are depicted in figures **2.9.a, 2.9.b** and **2.9.c** respectively.

A plot of transition temperature as a function of the number of carbon atoms in the terminal chain for parent compounds as well as fluorine substituted compounds are given in figures **2.10.a** and **2.10.b** respectively. Clearly, a smooth ascending curve for the mesophase-isotropic transition points is seen on increasing the *n*-alkoxy chain length as before. The parent compound **2.B.9** shows the widest thermal range of 17 °C for the SmA_{db} phase. In contrast to parent compounds, a very narrow range for the SmA_{db} phase and SmA_d phase was observed in the fluorine substituted compounds. Probably, this is due to the steric effect of the fluorine substituent.

2.3.2: X-Ray diffraction measurements

In order to examine the mesophase structure, X-ray diffraction measurements were carried out on the mesophases of compounds belonging to both series. XRD pattern of powder samples were obtained using Lindemann capillaries with diameter 0.7 mm. Samples were filled in the isotropic phase and the ends of the capillaries were sealed carefully. On irradiation, compound **2.A.6** at 140 °C gave two reflections in the small angle region with d-spacing d_1 = 54.5 Å and d_2 = 27.27 Å which are in the ratio 1 : 1/2 confirming a layer structure. In addition, a diffuse wide-angle peak with a maximum at 4.7 Å was obtained indicating a liquid-like in-plane order. The measured molecular length in the most extended form with an all *trans* conformation of the alkyl chain, L = 46.4 Å is less than the d-spacing obtained. The values obtained for compounds **2.A.3** to **2.A.7** are given in table **2.3.** It can be seen that the layer

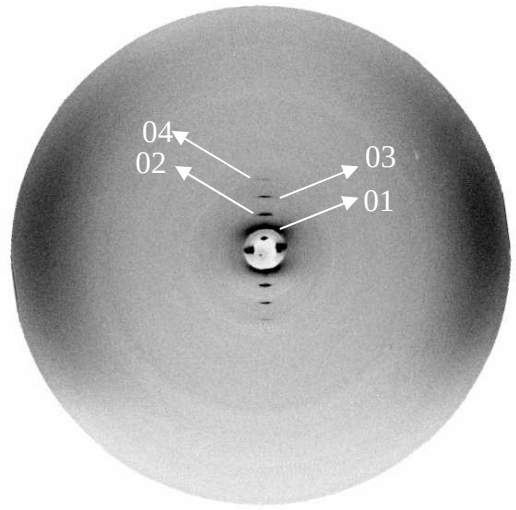

Figure 2.11: Oriented XRD pattern obtained for compound 2.A.6 in the SmA_dP_A phase at T = 140 °C.

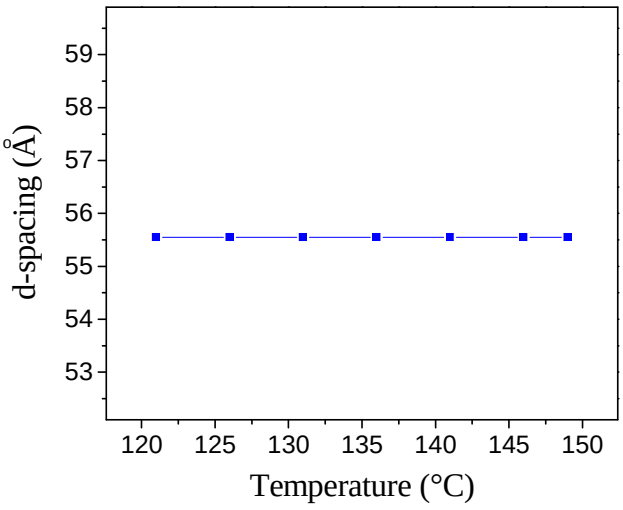

Figure 2.12: Plot of d spacing as a function of temperature for compound 2.A.7.

Table 2.3: Layer spacing data obtained from XRD for compounds of series 2.A and series 2.B

Compound	T/°C	d-spacings/Å			Measured molecular length/Å
		d_1	d_2	d_3	
2.A.3	135	50.39	25.2		
2.A.4	136	51.0	25.5		
2.A.5	140	52.74	26.39		
2.A.6	140	54.5	27.27		46.4
2.A.7	151	55.82			
	140	55.82			
2.B.3	103	46.65	23.35	15.3	
2.B.4	107	47.34	23.69	16.39	
2.B.5	110	49.52	24.78	17.07	
2.B.6	115	49.5	24.7	16.5	
2.B.8	120	52.8	26.4	17.6	44.8
2.B.9	124	54.2	27.1	18.0	
2.B.11	119	53.09	26.5	17.66	
	110	53.09	26.5	17.66	
2.B.12	123	53.36			
	115	53.36			

spacing d, is significantly larger than the calculated molecular length L, but less than 2L indicating a partial bilayer structure. It is well known [13-16] that in compounds containing a strongly polar terminal cyano group, the molecules organize themselves in an antiparallel fashion. Such an arrangement of molecules in the mesophase exist in these compounds as well.

The orthogonal arrangement of molecules in the mesophase was confirmed by carrying out XRD of oriented samples using the open drop method. Since the thermal range of the higher temperature uniaxial phase is small, the experiment was carried out in the lower temperature phase of compound **2.A.6**. The XRD pattern thus obtained for this material is given in figure **2.11.** It can be seen that the layer reflections upto the fourth order are positioned on the meridian while the diffuse wide-angle reflection is along the equator, clearly confirming the orthogonal arrangement of molecules. In addition, it was also found that the layer spacing did not change when a sample of **2.A.7** was cooled from the higher temperature uniaxial phase to the lower temperature biaxial phase as shown in figure **2.12.** It can be noticed that the d-spacing of mesophases are temperature independent.

Similar XRD measurements were carried out on the mesophase of compounds of series **2.B**. Three reflections in the small angle region were seen and the d values obtained are given in table **2.3**. Also, when a fluoro substituent was introduced *ortho* to the terminal cyano substituent, a uniaxial smectic phase was induced for compounds **2.B.11** to **2.B.12**. The XRD measurements clearly indicate a partial bilayer arrangement of molecules in both the mesophases.

2.3.3: Conoscopy

Further confirmation for the uniaxiality and biaxiality of the smectic A phases was obtained by conoscopy. For this, fairly well aligned samples were obtained in a cell constructed using an ITO coated conducting glass plate and an ordinary non-conducting glass plate, the inner surfaces of which were treated for homeotropic alignment. The ITO coated plate had an etched gap of ~1 mm across which an electric field could be applied. A sample of **2.A.7** was filled into such a cell (thickness 25 µm) and conoscopic observations made between crossed polarizers set

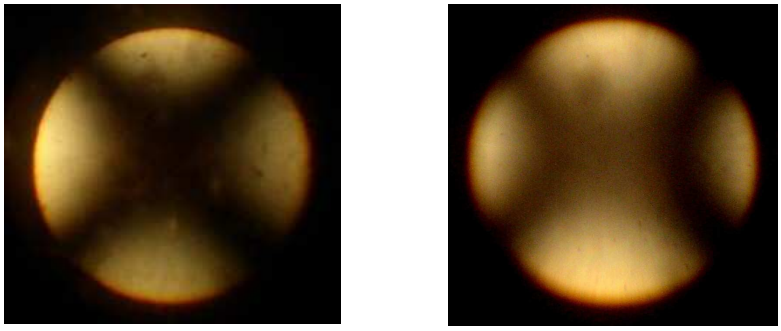

(a) **(b)**

Figure 2.13: Conoscopic patterns obtained for a homeotropically aligned sample of compound 2.A.7, (a) polar uniaxial smectic A_d phase at 150 °C; (b) polar biaxial smectic A_d phase at 147.2 °C.

at 45° to the direction in which the electric field could be applied. When the sample of **2.A.7** was cooled slowly from the isotropic phase, at 150 °C a uniaxial interference pattern was obtained as shown in figure **2.13.a**. From the uniaxial phase the sample was cooled further under the electric field (square-wave field, 100 V and frequency, 400 Hz). At a temperature of 147 °C a biaxial pattern in which the isogyres split was obtained and the gap between the isogyres increased as the temperature was lowered even further indicating that the lower temperature phase is indeed biaxial. Photomicrographs of the conoscopic patterns obtained for **2.A.7** in the uniaxial and biaxial phases are shown in figure **2.13.a** and **2.13.b** respectively.

2.3.4: Electro-optical studies

In order to examine if the mesophases exhibited by these compounds respond to an applied electric field, electro-optic studies using the standard triangular-wave field have been carried out. As an example, the switching behaviour of compound **2.A.7** is described here. A commercial cell (EHC, Japan) having a thickness of 8 µm and treated for homogeneous alignment was chosen. The sample was filled in this cell in the isotropic phase. When this

(a)

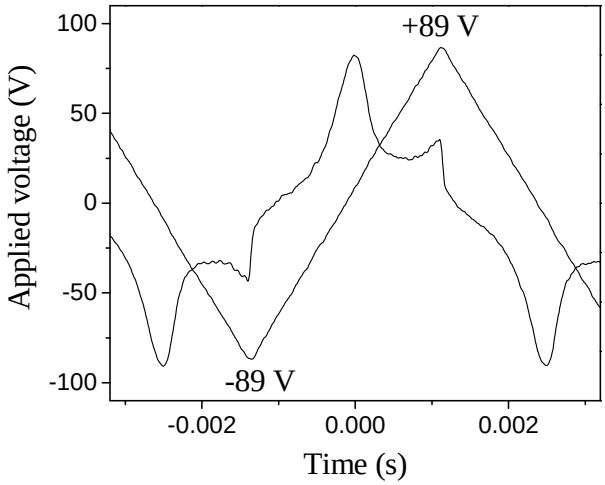

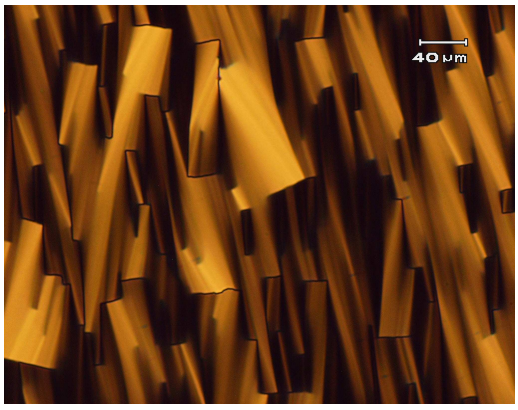

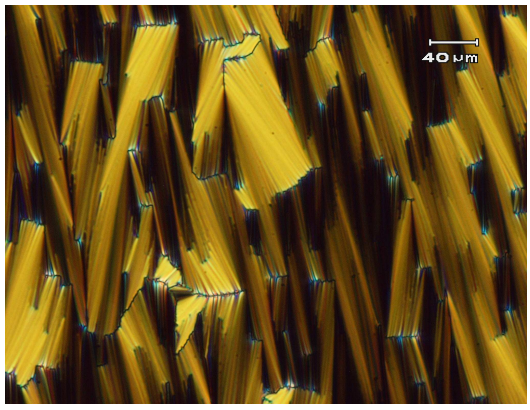

(b) **(c)**

Figure 2.14: (a) Switching current response obtained for compound 2.A.7 in the SmA_dP_R phase at T = 150 °C by applying a triangular-wave field, (b) & (c) photomicrographs at 178 V, 200 Hz and 0 V respectively, polarization value, $P_S \approx 36$ nC cm^{-2}; cell thickness, 8 µm.

sample was cooled slowly from isotropic phase into the smectic phase and triangular-wave electric field applied and above a threshold field (80 V), optical switching could be clearly seen in the higher temperature uniaxial phase. Thus, by applying appropriate voltage and frequency (178 V and 200 Hz), a single broad current peak was obtained for each half cycle. The current response as well as the textural change observed under these conditions in the field-on and field-

(a)

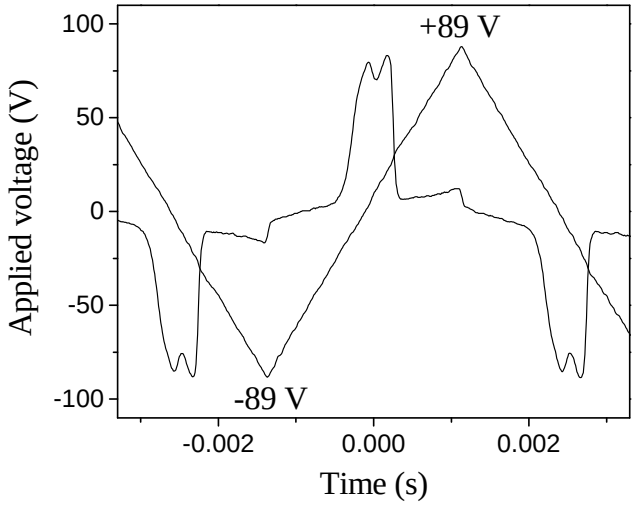

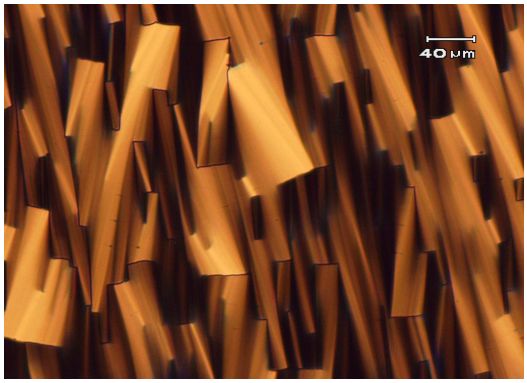

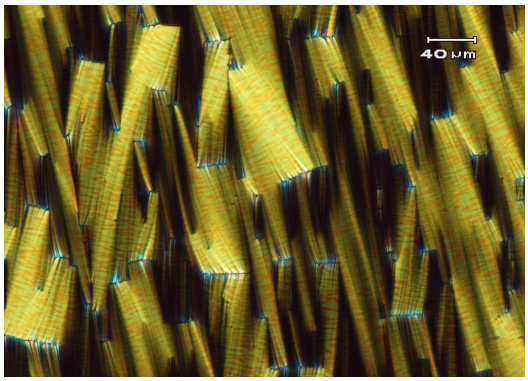

(b) **(c)**

Figure 2.15: (a) Switching current response obtained for compound 2.A.7 in the SmA_dP_A phase at T = 140 °C by applying a triangular-wave field, (b) & (c) photomicrographs (same region as in Figure 2.14.b & c) at 178 V, 200 Hz and 0 V respectively, polarization value, $P_S \approx 81$ nC cm^{-2}; cell thickness, 8 µm.

off states at 149 °C are shown in figure **2.14**. On cooling further into the lower temperature phase under the same conditions, the current response splits to give two peaks per half period of the applied field. This indicates an antiferroelectric behaviour of the lower temperature phase. The current response trace and the corresponding optical changes seen are shown in figure **2.15.**

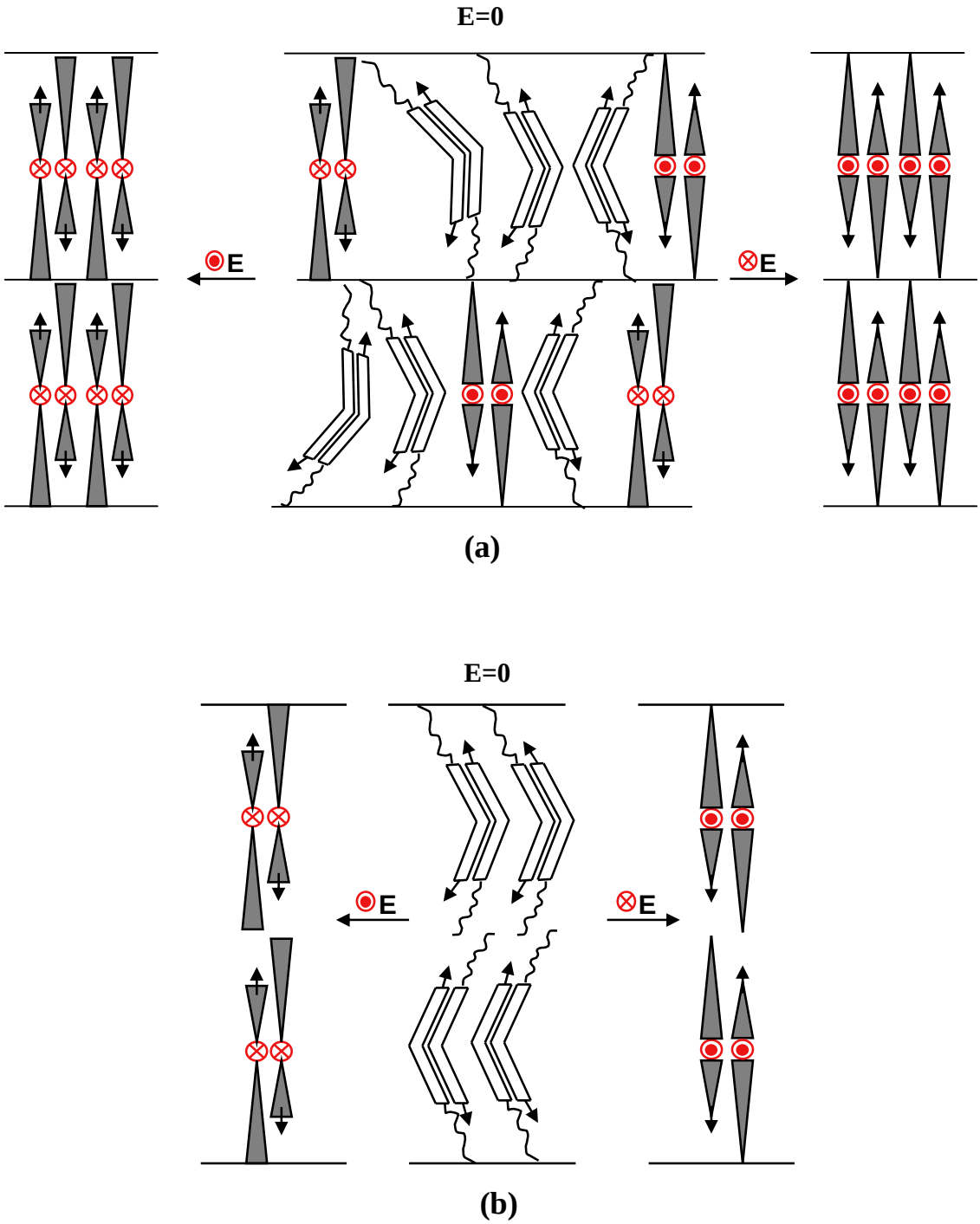

Figure 2.16: (a) Possible model for SmA_dP_R phase (after Gupta *et al.* [27]).
(b) Simple model of the field-induced antiferroelectric to ferroelectric transition. Black arrows connected to the arms of bent-cores stand for the strongly polar CN group (after Guo *et al.*[26]).

It is interesting to point out that Pociecha *et al.* [18] have described a structure formed by asymmetric bent-shaped molecules, which is layered, is optically uniaxial and has a non-tilted arrangement of molecules having a polar order with random direction of the layer polarization. They have ascribed this structure to the sign degeneracy of the difference in polarization directions in neighbouring layers and assigned the symbol $SmAP_R$ for this mesophase. The observation of a single broad polarization switching current peak for each half cycle of the applied field has been attributed to a field-induced alignment of dipoles from random orientation through the Langevin process. We observe similar switching current response in the higher temperature phase of compounds **2.A.6** and **2.A.7** which has a partial bilayer non-tilted structure. In analogy with what has been observed recently [18, 19] in other systems, we have assigned the symbol SmA_dP_R for this phase. In other words, the single broad current response peak suggests a polarization randomized inter layer structure. The possible model for switching in SmA_dP_R and SmA_dP_A phases are shown in figures **2.16.a** and **2.16.b** respectively. The detailed switching properties of both the orthogonal smectic phases were further confirmed experimentally as well as theoretically. Guo *et al.* [26] studied switching behaviour of SmA_dP_A phase of compound **2.A.6** by second-harmonic generation (SHG) and dielectric measurements. A simple theoretical model for the SmA_dP_R phase has recently been proposed by Gupta *et al.* [27].

Very interestingly, the mesophases of compounds belonging to series **2.B** did not respond to an applied electric field (as high as 400 V) although some textural change could be seen above 100 V. Based on optical textures, XRD and electro-optical studies, a possible model for the molecular organization in the SmA_{db} phase is shown in figure **2.17.**

Although the two series of compounds are isomeric, the electro-optical behaviour is very different and interesting.

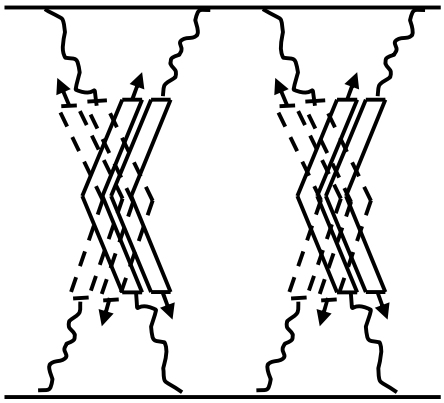

Figure 2.17: Schematic representation of the molecular arrangement in the apolar SmA_{db} phase exhibited by compounds of series 2.B. Black arrows connected to the arms of bent-cores stand for the strongly polar CN group (after Sadashiva *et al.* [15]).

2.4: Conclusions

Two new series of novel five-ring BC compounds have been synthesized. The compounds of series **2.A** are derived from 4-hydroxybiphenyl-3-carboxylic acid while those of series **2.B** are obtained from 3-hydroxybiphenyl-4-carboxylic acid. These represent the first examples of BC compounds derived from such moieties. While the biaxial smectic A phase has been observed in both series of compounds, the physical properties are quite contrasting. In series **2.A**, both the uniaxial and biaxial phases are polar in nature and in series **2.B**, both these phases are apolar. The introduction of a fluorine substituent *ortho* to the highly polar terminal cyano group has the effect of inducing a non-polar uniaxial partial bilayer smectic A phase. The most interesting result has been the occurrence of a transition between two polar partial bilayer orthogonal smectic phases, one of which is biaxial and the other uniaxial. The dark texture of the polar uniaxial partial bilayer smectic phase shown by compounds **2.A.6** and **2.A.7** are interesting as they exhibit a polarization randomized inter layer structure.

Experimental

General

In general, all synthesized intermediates as well as target compounds were purified by column chromatography on 60-120 mesh, ACME silica gel using appropriate solvents for elution. The compounds were further purified by repeated crystallization from suitable analytical grade solvents or mixture of solvents. The purity of the samples were checked using Merck Kieselgel $60F_{254}$ precoated thin layer chromatography (TLC). The chemical structure of the compounds was determined by standard spectroscopic techniques such as infrared (IR) spectroscopy, nuclear magnetic resonance (NMR) spectroscopy and elemental analysis. Infrared absorption spectra were recorded on a Shimadzu FTIR-8400 spectrophotometer, using nujol mull for intermediate compounds and KBr disk for target compounds. The wave number values are given in cm^{-1}. ^1H NMR spectra were recorded on a Bruker AMX 400 spectrometer, using tetramethylsilane (TMS) as an internal standard and deuterioacetone (CD_3COCD_3) or deuterated dimethylsulfoxide (DMSO-d_6) as solvents for intermediates and deuteriochloroform ($CDCl_3$) as solvent for target compounds. The chemical shift values (δ) are in parts per million (ppm) with respect to TMS. The elemental analyses were carried out for all the intermediates as well as final compounds using a Carlo-Erba 1106 analyzer and BBOT [2,5-bis(5-*tert*-butyl-benzoxazol-2-yl)-thiophene] and sulphanilamide as standards.

The mesomorphic behaviour of target compounds were examined using a combination of polarizing optical microscopy (POM), X-ray diffraction studies (XRD) and electro-optical measurements. The transition temperature and the associated enthalpy values of compounds were obtained from thermograms recorded on Perkin-Elmer, Model Pyris 1 differential scanning calorimeter (DSC), which was calibrated using indium as a standard. The rate of heating and cooling cycles were 5° min^{-1}. The optical textures of mesophases were observed using an Olympus BX50 polarizing optical microscope equipped with a Mettler FP82HT heating stage and a Mettler FP90 central processor.

The following two techniques were extensively used to examine the structure and polar properties of the mesophases exhibited by various BC compounds studied in this thesis.

(a) X-Ray diffraction measurements

(b) Electro-optical studies.

(a) X-Ray diffraction measurements

X-Ray diffraction measurements were carried out on samples in order to determine the structure of the mesophase. X-Ray diffraction (XRD) measurements were carried out on unoriented samples and in some cases on oriented samples. The powder samples were examined in Lindemann capillaries (diameter: 0.7 mm, wall thickness: 0.01 mm) which were cooled slowly from the isotropic state to the mesophase and irradiated. Oriented patterns were obtained by slow cooling of a drop of the sample on a glass plate from the isotropic state. In each case, the sample temperature was controlled to within ±0.1 °C.

The X-rays were generated by a Rigaku Ultrax-18 rotating anode generator. Thus the beam was monochromated to obtain radiation of wavelength λ = 1.54 Å (Cu-K_α) using graphite crystal. These X-rays were collimated through a double-slit arrangement and made to fall on the sample, which was taken in a sample holder. In each case, the sample temperature was controlled to within ±0.1 °C. The diffraction pattern of each sample was recorded on a Marresearch 2D image plate detector and a schematic representation of the X-ray set-up used is shown in figure **2.18.**

The layer spacing of the mesophase was calculated using Bragg's equation, $d = n\lambda / 2 \sin\theta$

Where, n = 1, (for first order reflection)

d = determined layer spacing

λ = 1.54 Å (characteristic wavelength of Cu-K_∞ radiation)

θ = Bragg's angle and can be calculated as $\theta = \frac{1}{2}\tan^{-1}\frac{R}{D}$

R = Radius of the diffraction pattern

D = Distance between the sample and the detector.

The tilt angle of the molecules in the mesophase can be calculated as

$\theta = \cos^{-1}\frac{d}{l}$ where, *l*-calculated molecular length.

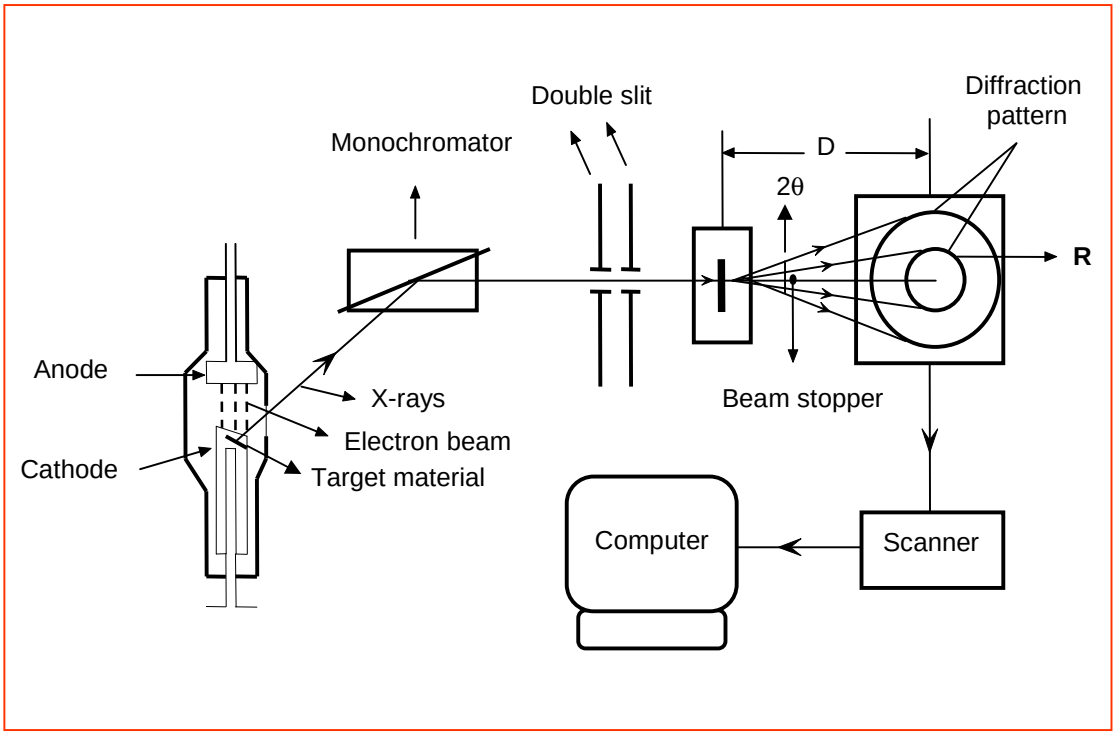

Figure 2.18: A block diagram showing the X-ray diffraction experimental set-up.

(b) Electro-optical studies

The electro-optical switching studies of samples were carried out using the standard triangular-wave method [28] in order to study the polar nature of the mesophase/s and to measure the spontaneous polarization value for the mesophase. A block diagram of the experimental set-up used is shown in figure **2.19**.

The switching studies were carried out either on home made cells and/or commercial cells obtained from EHC, Japan. These cells are made up of transparent glass plates and coated with indium tin oxide (ITO) for conduction. In order to obtain the planar alignment of samples, the inner surface of conducting plates were treated with polyimide and unidirectionally rubbed. The thickness of the cells was adjusted using Mylar spacers and the same was measured using interferometric techniques. The sample was filled in to the cell in the isotropic phase and

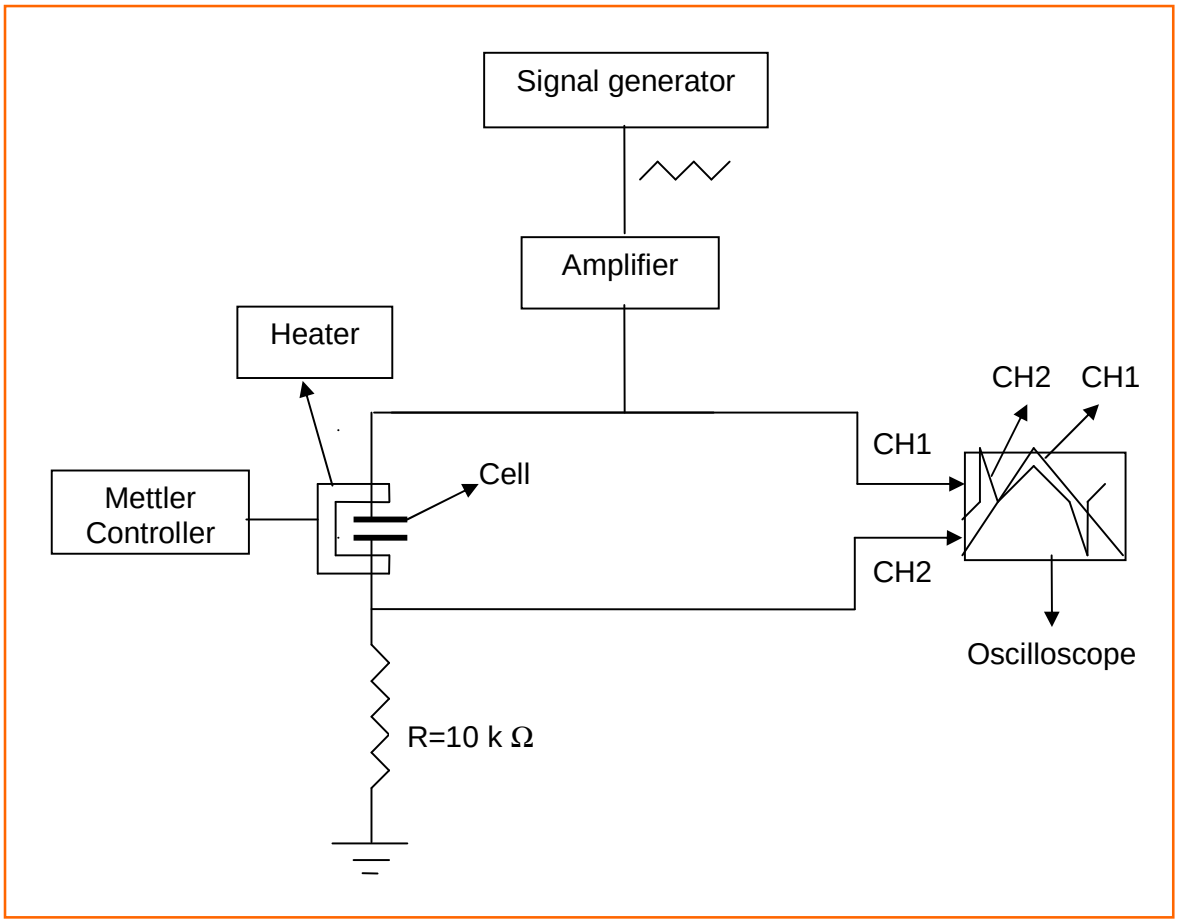

Figure 2.19: The block diagram of a circuit used for the measurement of polarization.

cooled slowly to get good alignment of the sample. The triangular wave of definite amplitude and frequency was produced by using a wave form generator (Wavetek model 39) which was amplified hundred times using an amplifier (Trek model 601-B). The output from the amplifier was divided into two channels CH1 and CH2. The waveform Channel CH1 was directly connected to the oscilloscope, which acted as a reference signal. The output signal CH2, from the sample was connected to the oscilloscope (Agilent 54621A) *via* a 10 kΩ resistance. The resultant curve obtained on the oscilloscope screen was a plot of switching current *versus* time.

The polarization value was calculated by integrating the area under the peaks obtained in the experiment using the relation

$$P \approx \frac{I \times t}{A}$$ where, I - current, t - time, A- cell area

Where, I = voltage (V in volts) / resistance (R in ohms)

t = response time in milliseconds.

The conoscopic experiments were performed in home made cells using a Leitz Ortholux-II POL BK microscope equipped with a heating stage (Mettler FP82) and a controller (FP80HT). The tilt sense or clinicity of the molecules in the mesophases was carried out by dc field experiments using a regulated dual dc power supply (Aplab, Model LD6401).

4-(Benzyloxy)biphenyl-3-carboxylic acid, 2.c

4-Benzyloxybiphenyl-3-carboxylic acid, **2.c** was prepared from methyl 4-hydroxylbiphenyl-3-carboxylate, **2.a** using benzyl chloride and anhydrous potassium carbonate in anhydrous butan-2-one. Thus, methyl 4-benzyloxybiphenyl-3-carboxylate (6.5 g, 20 mmol) was hydrolyzed in ethanol (100 mL), potassium hydroxide (3.43 g, 61.2 mmol) and water by refluxing overnight. The excess of ethanol was distilled off, reaction mixture cooled and poured into ice-cold water. The resulting solution was acidified with conc. HCl and heated on a water-bath for an hour and cooled. The white precipitate thus obtained was filtered off, washed several times with ice-cold water until the washings were neutral to litmus and dried. The material so obtained was crystallized using glacial acetic acid. Yield: 5.8 g (93%); mp 227.5-229 °C; IR (nujol) ν_{max}: 2922, 2852, 2712, 2616, 2559, 1703, 1679, 1606, 1571, 1454 cm^{-1}; ^1H NMR (400 MHz, DMSO-d_6) δ: 13.01 (s, 1H, Ar-COOH, exchangeable with D_2O), 8.12 (t, 1H, Ar-H), 7.86 (t, *J* = 7.72 Hz, 2H, Ar-H), 7.63 (d, *J* = 8.6 Hz, 2H, Ar-H), 7.54 (t, *J* = 7.76 Hz, 1H, Ar-H), 7.46 (d, *J* = 7.44 Hz, 2H, Ar-H), 7.39 (t, *J* = 7.32 Hz, 2H, Ar-H), 7.33 (d, *J* = 7.16 Hz, 1H, Ar-H), 7.11 (d, *J* = 8.64 Hz, 2H, Ar-H), 5.15 (s, 2H, Ar-O-CH_2-); Elemental analysis: $C_{20}H_{16}O_3$ requires C 78.93, H 5.29; found C 79.22, H 5.55%.

4-Cyanophenyl-4-hydroxybenzoate, 2.d

This was prepared following a procedure described in the literature [14]. mp 205-206 °C.

4-((4-Cyanophenoxy)carbonyl)phenyl -4′-(benzyloxy)biphenyl-3-carboxylate, 2.e

A mixture of 4-benzyloxybiphenyl-3-carboxylic acid, **2.c** (2 g, 6.57 mmol) and 4-cyanophenyl-4-hydroxybenzoate, **2.d** (1.57 g, 6.57 mmol) was stirred in anhydrous dichloromethane in the presence of a catalytic amount of 4-(*N*,*N*-dimethylamino)pyridine (DMAP). To this reaction mixture was added *N*,*N′*-dicyclohexylcarbodiimide (DCC, 1.49 g, 7.23 mmol) and stirred overnight at room temperature. The dicyclohexylurea formed was filtered off and washed with chloroform several times. Removal of the solvent from the filtrate gave a white material. This material was purified by column chromatography on silica gel using a mixture of 1% ethyl acetate in chloroform as an eluent. Evaporation of the solvent from the eluate gave compound **2.e** which was further crystallized from a mixture of chloroform and hexane. Yield: 2.59 g (75%); mp 202-204 °C; IR (nujol) ν_{max}: 2923, 2852, 2243, 1737, 1683, 1604, 1585, 1542, 1506, 1456 cm^{-1}; ^1H NMR (400 MHz, $CDCl_3$) δ: 8.39 (t, *J* = 1.68 Hz, 1H, Ar-H), 8.28 (d, *J* = 8.72 Hz, 2H, Ar-H), 8.14 (d, *J* = 7.88 Hz, 1H, Ar-H), 7.85 (d, *J* = 8.38 Hz, 1H, Ar-H), 7.75 (d, *J* = 8.68 Hz, 2H, Ar-H), 7.59 (d, *J* = 8.84 Hz, 3H, Ar-H), 7.46 (d, *J* = 8.52 Hz, 2H, Ar-H), 7.44-7.33 (m, 7H, Ar-H), 7.09 (d, *J* = 8.76, 2H, Ar-H), 5.13 (s, 2H, Ar-O-CH_2-); Elemental analysis: $C_{34}H_{23}NO_5$ requires C 77.7, H 4.4, N 2.66; found C 77.33, H 4.02, N 2.44%.

4-((4-Cyanophenoxy)carbonyl)phenyl-4′-hydroxybiphenyl-3-carboxylate, 2.f

Compound **2.e** (2.5 g, 4.76 mmol) was dissolved in 1,4-dioxane and 5% Pd-C catalyst (0.5 g) was added to it. The reaction mixture was stirred at 55 °C in an atmosphere of hydrogen until the required quantity of hydrogen was absorbed. The reaction mixture was filtered hot and removal of the solvent under reduced pressure gave a white material which was purified by column chromatography on silica gel using 5% acetone in chloroform as an eluent. Removal of solvent from the eluate followed by crystallization of the residue in a mixture of 1,4-dioxane and hexane provided pure compound **2.f**. Yield: 1.4 g (70%); mp 209-211 °C; IR (nujol) ν_{max}: 3377, 2923, 2852, 2243, 1728, 1683, 1598, 1577, 1558, 1456 cm^{-1}; ^1H NMR (400 MHz, CD_3COCD_3) δ: 8.76 (s, 1H, Ar-OH), 8.38 (t, *J* = 1.68 Hz, 1H, Ar-H), 8.31 (d, *J* = 8.72 Hz, 2H, Ar-H), 8.11 (d, *J* = 8.12 Hz, 1H, Ar-H), 7.96 (d, *J* = 8.56 Hz, 1H, Ar-H), 7.93 (d, *J* = 8.72 Hz, 2H, Ar-H), 7.66 (t, *J* = 7.76, 1H, Ar-H), 7.61 (d, *J* = 2.72, 2H, Ar-H), 7.6 (t, *J* = 1.92 Hz, 2H, Ar-H), 7.58 (d, *J* = 5.24 Hz, 2H, Ar-H), 6.97 (d, *J* = 8.76 Hz, 2H, Ar-H); Elemental analysis: $C_{27}H_{17}NO_5$ requires C 74.48, H 3.93, N 3.21; found C 74.15, H 3.62, N 3.54%.

4-*n*-Alkoxybenzoic acids, 2.g

These compounds were synthesized following a procedure described in the literature [29].

3-(Benzyloxy)biphenyl-4-carboxylic acid, 2.j

This was synthesized following a procedure described for the preparation of compound **2.c** using methyl 3-hydroxybiphenyl-4-carboxylate, **2.h** as starting material. Yield: (91%); mp 187.5-189 °C; IR (nujol) ν_{max}: 2922, 2852, 2710, 2667, 2551, 1681, 1610, 1596, 1568, 1454, 1425 cm^{-1}; ^1H NMR (400 MHz, DMSO-d_6) δ: 8.1 (d, *J* = 8.42 Hz, 2H, Ar-H), 7.79 (d, *J* = 8.42 Hz, 2H, Ar-H), 7.51 (d, *J* = 7.19 Hz, 1H, Ar-H), 7.43-7.29 (m, 7H, Ar-H), 7.07 (d, *J* = 7.93 Hz, 1H, Ar-H), 5.22 (s, 2H, Ar-O-CH_2-); Elemental analysis: $C_{20}H_{16}O_3$ requires C 78.93, H 5.29; found C 79.33, H 5.65%.

4-*n*-alkoxybenzoyloxy-4-benzoic acid, 2.m

Two ring carboxylic acids, **2.m** were prepared in two steps following a procedure similar to that described in the literature for 4-*n*-dodecyloxybenzoyloxy-4-benzoic acid [30]. As an example, detailed procedure and analytical data are given for compound **2.m (*n*=18)** and the transition temperatures obtained for other compounds are given in table **2.4.**

Benzyl 4-(4-*n*-octadecyloxybenzoyloxy)benzoate, 2.l (*n* = 18)

This was synthesized following a procedure described for the preparation of compound **2.e** using 4-*n*-octadecyloxybenzoic acid, **2.g** (3 g, 7.69 mmol), benzyl 4-hydroxybenzoate, **2.k** (1.75 g, 7.69 mmol) and DCC (1.74 g, 8.46 mmol) in the presence of a catalytic amount of DMAP in dichloromethane. Yield: 4 g (86.5%); mp 79-80 °C; IR (nujol) ν_{max}: 2920, 2850, 2667, 1730, 1716, 1697, 1683, 1541, 1508, 1456, 1377, 1338 cm^{-1}; ^1H NMR (400 MHz, $CDCl_3$) δ: 8.16-8.12 (m, 4H, Ar-H), 7.46-7.35 (m, 5H, Ar-H), 7.29 (d, *J* = 8.64 Hz, 2H, Ar-H), 6.97 (d, *J* = 8.8 Hz, 2H, Ar-H), 5.38 (s, 2H, Ar-CH_2-COO-), 4.03 (t, *J* = 6.48 Hz, 2H, Ar-O-CH_2-), 1.85-1.78 (quin, *J* = 6.5 Hz, 2H, Ar-O-CH_2-C$\underline{H}_2$-), 1.47-1.26 (m, 30H, -$(CH_2)_{15}$-), 0.88 (t, *J* = 6.32 Hz, 3H, -CH_3); Elemental analysis: $C_{39}H_{52}O_5$ requires C 77.76, H 8.72; found C 77.92, H 8.38%.

4-*n*-Octadecyloxybenzoyloxy-4-benzoic acid, 2.m (*n* = 18)

This was synthesized following a procedure described for the preparation of compound **2.f** using benzyl 4-(4-*n*-octadecyloxybenzoyloxy)benzoate, **2.l** as starting material. Yield: (86%), transition temperature: Cr 118.5 °C SmC 212 °C I; IR (nujol) ν_{max}: 2922, 2852, 2553, 1732, 1683, 1602, 1508, 1456, 1375, 1261, 1217 cm^{-1}; ^1H NMR (400 MHz, CD_3COCD_3) δ: 8.14 (d, *J* = 8.8 Hz, 4H, Ar-H), 7.42 (d, *J* = 8.4 Hz, 2H, Ar-H), 7.12 (d, *J* = 8 Hz, 2H, Ar-H), 4.15 (t, *J* = 6.4 Hz, 2H, Ar-O-CH_2-), 1.86-1.79 (quin, *J* = 6.8 Hz, 2H, Ar-O-CH_2-C$\underline{H}_2$-), 1.54-1.28 (m, 30H, -$(CH_2)_{15}$-), 0.89 (t, *J* = 6.8 Hz, 3H, -CH_3); Elemental analysis: $C_{32}H_{46}O_5$ requires C 75.25, H 9.07; found C 75.18, H 8.96%.

Table 2.4: Transition temperatures of 4-*n*-alkoxybenzoyloxy-4-benzoic acids, 2.m

Compound	*n*	Transition temperature (°C)
2.m.1	8	Cr 141.0 SmC 177.5 N 236.5 I
2.m.2	10	Cr 132.0 SmC 202.5 N 229.5 I
2.m.3	11	Cr 125.0 SmC 207.5 N 225.5 I
2.m.4	12	Cr 122.5 SmC 211.5 N 223.5 I
2.m.5	13	Cr 121.5 SmC 213.5 N 220.5 I
2.m.6	14	Cr 120.5 SmC 215.0 N 218.5 I
2.m.7	15	Cr 121.0 SmC 215.5 I
2.m.8	16	Cr 120.5 SmC 215.0 I
2.m.9	18	Cr 118.5 SmC 212.0 I
2.m.10	20	Cr 118.5 SmC 209.5 I

4-Cyanophenyl-3′-(benzyloxy)biphenyl-4-carboxylate, 2.o (X = H)

This was synthesized following a procedure described for the preparation of compound **2.e** using 3-benzyloxybiphenyl-4-carboxylic acid, **2.j** and 4-cyanophenol, **2.n.** Yield: (78%); mp 118.5-120 °C; IR (nujol) ν_{max}: 3064, 3033, 2922, 2852, 2227, 1733, 1716, 1697, 1602, 1581, 1558, 1480, 1456 cm^{-1}; ^1H NMR (400 MHz, $CDCl_3$) δ: 8.24 (d, *J* = 8.35 Hz, 2H, Ar-H), 7.74 (dd, J_1 = 3.12 Hz, J_2 = 8.4 Hz, 5H, Ar-H), 7.47 (d, *J* = 7.06 Hz, 2H, Ar-H), 7.43-7.33 (m, 7H,

Ar-H), 7.04 (d, *J* = 6.91, 1H, Ar-H), 5.15 (s, 2H, Ar-O-CH_2-); Elemental analysis: $C_{27}H_{19}NO_3$ requires C 79.99, H 4.72, N 3.45; found C 80.38, H 4.52, N 3.34%.

4-Cyanophenyl-3′-hydroxybiphenyl-4-carboxylate, 2.p (X = H)

This was synthesized following a procedure described for the preparation of compound **2.f** using compound **2.o.** Yield: (70%); Cr 197.5 N 217 °C I; IR (nujol) ν_{max}: 3334, 2920, 2852, 2250, 1919, 1732, 1602, 1585, 1456, 1377 cm^{-1}; ^1H NMR (400 MHz, CD_3COCD_3) δ: 8.56 (s, 1H, Ar-OH), 8.24 (d, *J* = 8.57 Hz, 2H, Ar-H), 7.93 (d, *J* = 8.79 Hz, 2H, Ar-H), 7.85 (d, *J* = 8.61 Hz, 2H, Ar-H), 7.59 (d, *J* = 8.77 Hz, 2H, Ar-H), 7.34 (t, *J* = 7.84, 1H, Ar-H), 7.22 (d, *J* = 8.58 Hz, 2H, Ar-H), 6.92 (d, *J* = 8.10 Hz, 1H, Ar-H); Elemental analysis: $C_{20}H_{13}NO_3$ requires C 76.18, H 4.15, N 3.91; found C 75.83, H 4.09, N 3.58%.

4-Cyano-3-fluorophenyl-3′-(benzyloxy)biphenyl-4-carboxylate, 2.o (X = F)

This was synthesized following a procedure described for the preparation of compound **2.e** using 3-benzyloxybiphenyl-4-carboxylic acid, **2.j** and 3-fluoro-4-cyanophenol, **2.n**. Yield: (78%); mp 102-104 °C; IR (nujol) ν_{max}: 3064, 2923, 2852, 2235, 1737, 1716, 1612, 1604, 1506, 1488, 1456 cm^{-1}; ^1H NMR (400 MHz, $CDCl_3$) δ: 8.22 (d, *J* = 8.3 Hz, 2H, Ar-H), 7.73 (d, *J* = 8.31 Hz, 3H, Ar-H), 7.47 (d, *J* = 7.18 Hz, 2H, Ar-H), 7.43 (t, *J* = 7.47 Hz, 3H, Ar-H), 7.36 (d, *J* = 7.17 Hz, 1H, Ar-H), 7.27-7.21 (m, 4H, Ar-H), 7.05 (d, *J* = 7.19 Hz, 1H, Ar-H), 5.15 (s, 2H, Ar-O-CH_2-); Elemental analysis: $C_{27}H_{18}FNO_3$ requires C 76.58, H 4.28, N 3.3; found C 76.20, H 4.39, N 3.68%.

4-Cyano-3-fluorophenyl-3′-hydroxybiphenyl-4-carboxylate, 2.p (X = F)

This was synthesized following a procedure described for the preparation of compound **2.f** using compound **2.o.** Yield: (65%); mp 183-185 °C; IR (nujol) ν_{max}: 3373, 2922, 2854, 2250, 1735, 1604, 1587, 1558, 1456, 1377 cm^{-1}; ^1H NMR (400 MHz, DMSO-d_6) δ: 9.7 (s, 1H, Ar-OH, D_2O exchangeable), 8.19 (d, *J* = 8.1 Hz, 2H, Ar-H), 8.1 (t, *J* = 8.4 Hz, 1H, Ar-H), 7.86 (d, *J* = 8.4 Hz, 2H, Ar-H), 7.74 (d, *J* = 8.4 Hz, 2H, Ar-H), 7.48 (d, *J* = 6.6 Hz, 1H, Ar-H), 7.32 (t, *J* = 8.1 Hz, 1H, Ar-H), 7.18 (d, *J* = 7.5 Hz, 1H, Ar-H), 6.86 (d, *J* = 5.7, 1H, Ar-H); Elemental analysis: $C_{20}H_{12}FNO_3$ requires C 72.07, H 3.62, N 4.2; found C 71.73, H 3.76, N 4.38%.

4-((4-Cyanophenoxy)carbonyl)phenyl-4′-(4-*n*-dodecyloxybenzoyloxy)biphenyl-3-carboxylate, 2.A.1

This was synthesized following a procedure described for the preparation of compound **2.e** using compound **2.f** and 4-*n*-octyloxybenzoic acid **2.g.** Yield: (70%); mp 147 °C; IR (KBr) ν_{max}: 3067, 2918, 2848, 2243, 1735, 1733, 1604, 1577, 1508, 1473 cm^{-1}; ^1H NMR (400 MHz, $CDCl_3$) δ: 8.44 (t, *J* = 1.64 Hz, 1H, Ar-H), 8.3 (d, *J* = 8.72 Hz, 2H, Ar-H), 8.2 (d, *J* = 7.82 Hz, 1H, Ar-H), 8.16 (d, *J* = 8.84 Hz, 2H, Ar-H), 7.9 (d, *J* = 8 Hz, 1H, Ar-H), 7.75 (d, *J* = 6.73 Hz, 2H, Ar-H), 7.71 (d, *J* = 8.6 Hz, 2H, Ar-H), 7.63 (t, *J* = 7.73 Hz, 1H, Ar-H), 7.44 (d, *J* = 8.7 Hz, 2H, Ar-H), 7.39 (d, *J* = 8.71, 2H, Ar-H), 7.33 (d, *J* = 8.59 Hz, 2H, Ar-H), 6.98 (d, *J* = 8.9 Hz, 2H, Ar-H), 4.05 (t, *J* = 6.5 Hz, 2H, Ar-O-CH_2-), 1.86-1.79 (quin, *J* = 6.61 Hz, 2H, Ar-O-CH_2-C$\underline{H}_2$-), 1.5-1.26 (m, 18H, -$(CH_2)_9$-), 0.87 (t, *J* = 6.58 Hz, 3H, -CH_3); Elemental analysis: $C_{46}H_{45}NO_7$ requires C 76.33, H 6.27, N 1.94; found C 75.97, H 6.1, N 1.77%.

4-((4-Cyanophenoxy)carbonyl)phenyl-4′-(4-*n*-tridecyloxybenzoyloxy)biphenyl-3-carboxylate, 2.A.2

Yield: (75%); mp 134.5 °C; IR (KBr) ν_{max}: 3078, 2922, 2852, 2241, 1737, 1728, 1606, 1508, 1454, 1377 cm^{-1}; ^1H NMR (400 MHz, $CDCl_3$) δ: 8.44 (t, *J* = 1.66 Hz, 1H, Ar-H), 8.3 (d, *J* = 8.74 Hz, 2H, Ar-H), 8.21 (d, *J* = 7.8 Hz, 1H, Ar-H), 8.17 (d, *J* = 8.88 Hz, 2H, Ar-H), 7.9 (d, *J* = 8.03 Hz, 1H, Ar-H), 7.76 (d, *J* = 6.75 Hz, 2H, Ar-H), 7.7 (d, *J* = 8.6 Hz, 2H, Ar-H), 7.63 (t, *J* = 7.73 Hz, 1H, Ar-H), 7.44 (d, *J* = 8.74 Hz, 2H, Ar-H), 7.39 (d, *J* = 8.73, 2H, Ar-H), 7.34 (d, *J* = 8.64 Hz, 2H, Ar-H), 6.99 (d, *J* = 9 Hz, 2H, Ar-H), 4.05 (t, *J* = 6.8 Hz, 2H, Ar-O-CH_2-), 1.86-1.79 (quin, *J* = 7 Hz, 2H, Ar-O-CH_2-C$\underline{H}_2$-), 1.53-1.25 (m, 20H, -$(CH_2)_{10}$-), 0.88 (t, *J* = 6.64 Hz, 3H, -CH_3); Elemental analysis: $C_{47}H_{47}NO_7$ requires C 76.51, H 6.41, N 1.89; found C 76.6, H 6.42, N 1.72%.

4-((4-Cyanophenoxy)carbonyl)phenyl-4′-(4-*n*-tetradecyloxybenzoyloxy)biphenyl-3-carboxylate, 2.A.3

Yield: (72%); mp 135.5 °C; IR (KBr) ν_{max}: 3103, 3068, 2918, 2848, 2241, 1743, 1737, 1608, 1508, 1473 cm^{-1}; ^1H NMR (400 MHz, $CDCl_3$) δ: 8.44 (t, *J* = 1.66 Hz, 1H, Ar-H), 8.30 (d, *J* = 8.72 Hz, 2H, Ar-H), 8.21 (d, *J* = 7.84 Hz, 1H, Ar-H), 8.17 (d, *J* = 8.9 Hz, 2H, Ar-H), 7.91 (d, *J* = 8.08 Hz, 1H, Ar-H), 7.78 (d, *J* = 6.75 Hz, 2H, Ar-H), 7.71 (d, *J* = 8.6 Hz, 2H, Ar-H), 7.63 (t,

J = 7.76 Hz, 1H, Ar-H), 7.44 (d, *J* = 8.74 Hz, 2H, Ar-H), 7.39 (d, *J* = 8.71, 2H, Ar-H), 7.33 (d, *J* = 8.59 Hz, 2H, Ar-H), 6.99 (d, *J* = 8.9 Hz, 2H, Ar-H), 4.05 (t, *J* = 6.54 Hz, 2H, Ar-O-CH_2-), 1.86-1.79 (quin, *J* = 6.67 Hz, 2H, Ar-O-CH_2-C$\underline{H}_2$-), 1.60-1.26 (m, 22H, -$(CH_2)_{11}$-), 0.88 (t, *J* = 7 Hz, 3H, -CH_3); Elemental analysis: $C_{48}H_{49}NO_7$ requires C 76.68, H 6.56, N 1.86; found C 76.79, H 6.38, N 2.13%.

4-((4-Cyanophenoxy)carbonyl)phenyl-4′-(4-*n*-pentadecyloxybenzoyloxy)biphenyl-3-carboxylate, 2.A.4

Yield: (70%); mp 134.5 °C; IR (KBr) ν_{max}: 3070, 2922, 2852, 2243, 1737, 1733, 1604, 1558, 1506, 1473, 1454 cm^{-1}; ^{1}H NMR (400 MHz, $CDCl_3$) δ: 8.44 (t, *J* = 1.68 Hz, 1H, Ar-H), 8.29 (d, *J* = 8.8 Hz, 2H, Ar-H), 8.21 (d, *J* = 8 Hz, 1H, Ar-H), 8.17 (d, *J* = 8.84 Hz, 2H, Ar-H), 7.90 (d, 1H, *J* = 8.03 Hz, 1H, Ar-H), 7.76 (d, *J* = 6.72 Hz, 2H, Ar-H), 7.7 (d, *J* = 8.6 Hz, 2H, Ar-H), 7.63 (t, *J* = 7.8 Hz, 1H, Ar-H), 7.44 (d, *J* = 8.7 Hz, 2H, Ar-H), 7.39 (d, *J* = 8.7, 2H, Ar-H), 7.34 (d, *J* = 8.6 Hz, 2H, Ar-H), 6.98 (d, *J* = 9 Hz, 2H, Ar-H), 4.05 (t, *J* = 6.6 Hz, 2H, Ar-O-CH_2-), 1.84-1.8 (quin, *J* = 6.92 Hz, 2H, Ar-O-CH_2-C$\underline{H}_2$-), 1.54-1.26 (m, 24H, -$(CH_2)_{12}$-), 0.88 (t, *J* = 6.68 Hz, 3H, -CH_3); Elemental analysis: $C_{49}H_{51}NO_7$ requires C 76.84, H 6.71, N 1.83; found C 76.78, H 7.05, N 1.82%.

4-((4-Cyanophenoxy)carbonyl)phenyl-4′-(4-*n*-hexadecyloxybenzoyloxy)biphenyl-3-carboxylate, 2.A.5

Yield: (73%); mp 135 °C; IR (KBr) ν_{max}: 3077, 2922, 2854, 2243, 1737, 1733, 1604, 1556, 1508, 1474 cm^{-1}; ^{1}H NMR (400 MHz, $CDCl_3$) δ: 8.44 (t, *J* = 1.68 Hz, 1H, Ar-H), 8.30 (d, *J* = 8.7 Hz, 2H, Ar-H), 8.21 (d, *J* = 6.52 Hz, 1H, Ar-H), 8.17 (d, *J* = 8.8 Hz, 2H, Ar-H), 7.91 (d, *J* = 8.03 Hz, 1H, Ar-H), 7.77 (d, *J* = 6.75 Hz, 2H, Ar-H), 7.71 (d, *J* = 8.6 Hz, 2H, Ar-H), 7.63 (t, *J* = 7.73 Hz, 1H, Ar-H), 7.44 (d, *J* = 8.74 Hz, 2H, Ar-H), 7.39 (d, *J* = 8.71, 2H, Ar-H), 7.33 (d, *J* = 8.59 Hz, 2H, Ar-H), 6.99 (d, *J* = 8.8 Hz, 2H, Ar-H), 4.05 (t, *J* = 6.57 Hz, 2H, Ar-O-CH_2-), 1.87-1.79 (quin, *J* = 6.64 Hz, 2H, Ar-O-CH_2-C$\underline{H}_2$-), 1.52-1.26 (m, 26H, -$(CH_2)_{13}$-), 0.88 (t, *J* = 6.69 Hz, 3H, -CH_3); Elemental analysis: $C_{50}H_{53}NO_7$ requires C 77.0, H 6.84, N 1.79; found C 76.74, H 7.17, N 1.98%.

4-((4-Cyanophenoxy)carbonyl)phenyl-4′-(4-*n*-octadecyloxybenzoyloxy)biphenyl-3-carboxylate, 2.A.6

Yield: (75%); mp 134.5 °C; IR (KBr) ν_{max}: 3101, 3070, 2918, 2848, 2243, 1735, 1733, 1604, 1577, 1508, 1473 cm^{-1}; ^1H NMR (400 MHz, $CDCl_3$) δ: 8.44 (t, *J* = 1.66 Hz, 1H, Ar-H), 8.3 (d, *J* = 8.72 Hz, 2H, Ar-H), 8.20(d, *J* = 7.8 Hz, 1H, Ar-H), 8.16 (d, *J* = 8.88 Hz, 2H, Ar-H), 7.9 (d, *J* = 8.03 Hz, 1H, Ar-H), 7.75 (d, *J* = 6.75 Hz, 2H, Ar-H), 7.71 (d, *J* = 8.6 Hz, 2H, Ar-H), 7.63 (t, *J* = 7.73 Hz, 1H, Ar-H), 7.44 (d, *J* = 8.74 Hz, 2H, Ar-H), 7.39 (d, *J* = 8.71, 2H, Ar-H), 7.33 (d, *J* = 8.59 Hz, 2H, Ar-H), 6.98 (d, *J* = 8.9 Hz, 2H, Ar-H), 4.05 (t, *J* = 6.5 Hz, 2H, Ar-O-CH_2-), 1.86-1.79 (quin, *J* = 6.63 Hz, 2H, Ar-O-CH_2-C$\underline{H}_2$-), 1.5-1.26 (m, 30H, -$(CH_2)_{15}$-), 0.87 (t, *J* = 6.58 Hz, 3H, -CH_3); Elemental analysis: $C_{52}H_{57}NO_7$ requires C 77.3, H 7.1, N 1.73; found C 77.03, H 7.2, N 1.97%.

4-((4-Cyanophenoxy)carbonyl)phenyl-4′-(4-*n*-icosyloxybenzoyloxy)biphenyl-3-carboxylate, 2.A.7

Yield: (70%); mp 134.5 °C; IR (KBr) ν_{max}: 3070, 2918, 2848, 2243, 1735, 1701, 1606, 1569, 1508, 1473, 1458 cm^{-1}; ^1H NMR (400 MHz, $CDCl_3$) δ: 8.44 (t, *J* = 1.56 Hz, 1H, Ar-H), 8.3 (d, *J* = 8.71 Hz, 2H, Ar-H), 8.21 (d, *J* = 7.4 Hz, 1H, Ar-H), 8.18 (d, *J* = 8.8 Hz, 2H, Ar-H), 7.91 (d, *J* = 8 Hz, 1H, Ar-H), 7.72 (d, *J* = 6.73 Hz, 2H, Ar-H), 7.7 (d, *J* = 8.6 Hz, 2H, Ar-H), 7.65 (t, *J* = 7.73 Hz, 1H, Ar-H), 7.44 (d, *J* = 8.74 Hz, 2H, Ar-H), 7.4 (d, *J* = 8.71, 2H, Ar-H), 7.35 (d, *J* = 8.59 Hz, 2H, Ar-H), 6.99 (d, *J* = 8.9 Hz, 2H, Ar-H), 4.05 (t, *J* = 6.5 Hz, 2H, Ar-O-CH_2-), 1.84-1.81 (quin, *J* = 6.6 Hz, 2H, Ar-O-CH_2-C$\underline{H}_2$-), 1.55-1.26 (m, 34H, -$(CH_2)_{17}$-), 0.87 (t, *J* = 7 Hz, 3H, -CH_3); Elemental analysis: $C_{54}H_{61}NO_7$ requires C 77.58, H 7.34, N 1.67; found C 77.65, H 7.35, N 1.79%.

4-Cyanophenyl-3′-(4-(4-*n*-decyloxybenzoyloxy)benzoyloxy)biphenyl-4-carboxylate, 2.B.1 (X = H)

This was synthesized following a procedure described for the preparation of compound **2.e** using compound **2.p** and compound **2.m.** Yield: (70%); mp 115.5 °C; IR (KBr) ν_{max}: 3101, 3065, 2922, 2852, 2229, 1737, 1724, 1602, 1504, 1461, 1377 cm^{-1}; ^1H NMR (400 MHz, $CDCl_3$) δ: 8.32 (d, *J* = 8.76 Hz, 2H, Ar-H), 8.27 (d, *J* = 8.5 Hz, 2H, Ar-H), 8.16 (d, *J* = 8.6 Hz, 2H, Ar-H), 7.77 (dd, J_1 = 2 Hz, J_2 = 4.08 Hz, 4H, Ar-H), 7.59-7.52 (m, 3H, Ar-H), 7.4 (dd, J_1 = 1.98

Hz, J_2 = 6.78 Hz, 4H, Ar-H), 7.33-7.29 (m, 1H, Ar-H), 6.99 (d, J = 9 Hz, 2H, Ar-H), 4.05 (t, J = 6.74 Hz, 2H, Ar-O-CH_2-), 1.87-1.79 (quin, J = 7.46 Hz, 2H, Ar-O-CH_2-C$\underline{H}_2$-), 1.52-1.28 (m, 14H, -$(CH_2)_7$-), 0.89 (t, J = 6.62 Hz, 3H, -CH_3); Elemental analysis: $C_{44}H_{41}NO_7$ requires C 75.95, H 5.93, N 2.01; found C 75.95, H 6.28, N 1.73%.

4-Cyanophenyl-3′-(4-(4-*n*-undecyloxybenzoyloxy)benzoyloxy)biphenyl-4-carboxylate, 2.B.2 (X = H)

Yield: (74%); mp 104 °C; IR (KBr) ν_{max}: 3092, 3070, 2920, 2848, 2229, 1737, 1728, 1602, 1508, 1465, 1373 cm^{-1}; ^{1}H NMR (400 MHz, $CDCl_3$) δ: 8.32 (d, J = 8.71 Hz, 2H, Ar-H), 8.27 (d, J = 8.6 Hz, 2H, Ar-H), 8.16 (d, J = 8.79 Hz, 2H, Ar-H), 7.77 (dd, J_1 = 2.05 Hz, J_2 = 4.06 Hz, 4H, Ar-H), 7.59-7.52 (m, 3H, Ar-H), 7.4 (dd, J_1 = 2.15 Hz, J_2 = 6.64 Hz, 4H, Ar-H), 7.32-7.28 (m, 1H, Ar-H), 6.99 (d, J = 8.88 Hz, 2H, Ar-H), 4.06 (t, J = 6.6 Hz, 2H, Ar-O-CH_2-), 1.85-1.79 (quin, J = 7.56 Hz, 2H, Ar-O-CH_2-C$\underline{H}_2$-), 1.52-1.27 (m, 16H, -$(CH_2)_8$-), 0.88 (t, J = 6.64 Hz, 3H, -CH_3); Elemental analysis: $C_{45}H_{43}NO_7$ requires C 76.14, H 6.1, N 1.97; found C 76.44, H 5.89, N 1.59%.

4-Cyanophenyl-3′-(4-(4-*n*-dodecyloxybenzoyloxy)benzoyloxy)biphenyl-4-carboxylate, 2.B.3 (X = H)

Yield: (78%); mp 118 °C; IR (KBr) ν_{max}: 3095, 3070, 2923, 2852, 2229, 1735, 1728, 1604, 1502, 1460, 1377 cm^{-1}; ^{1}H NMR (400 MHz, $CDCl_3$) δ: 8.32 (d, J = 8.6 Hz, 2H, Ar-H), 8.26 (d, J = 8.2 Hz, 2H, Ar-H), 8.16 (d, J = 8.8 Hz, 2H, Ar-H), 7.77 (dd, J_1 = 2.05 Hz, J_2 = 4.06 Hz, 4H, Ar-H), 7.59-7.52 (m, 3H, Ar-H), 7.39 (dd, J_1 = 1.96 Hz, J_2 = 6.74 Hz, 4H, Ar-H), 7.33-7.29 (m, 1H, Ar-H), 6.99 (d, J = 8.9 Hz, 2H, Ar-H), 4.05 (t, J = 6.74 Hz, 2H, Ar-O-CH_2-), 1.87-1.79 (quin, J = 7.8 Hz, 2H, Ar-O-CH_2-C$\underline{H}_2$-), 1.53-1.27 (m, 18H, -$(CH_2)_9$-), 0.88 (t, J = 6.8 Hz, 3H, -CH_3); Elemental analysis: $C_{46}H_{45}NO_7$ requires C 76.33, H 6.26, N 1.93; found C 76.54, H 5.88, N 1.9%.

4-Cyanophenyl-3′-(4-(4-*n*-tridecyloxybenzoyloxy)benzoyloxy)biphenyl-4-carboxylate, 2.B.4 (X = H)

Yield: (75%); mp 122 °C; IR (KBr) ν_{max}: 3098, 3068, 2922, 2852, 2229, 1743, 1733, 1606, 1506, 1456, 1377 cm^{-1}; ^{1}H NMR (400 MHz, $CDCl_3$) δ: 8.31 (d, J = 8.59 Hz, 2H, Ar-H),

8.27 (d, *J* = 8 Hz, 2H, Ar-H), 8.17 (d, *J* = 8.79 Hz, 2H, Ar-H), 7.77 (dd, J_1 = 2.08 Hz, J_2 = 4.06 Hz, 4H, Ar-H), 7.59-7.52 (m, 3H, Ar-H), 7.4 (dd, J_1 = 2.2 Hz, J_2 = 6.8 Hz, 4H, Ar-H), 7.32-7.28 (m, 1H, Ar-H), 6.99 (d, *J* = 8.84 Hz, 2H, Ar-H), 4.05 (t, *J* = 6.54 Hz, 2H, Ar-O-CH_2-), 1.87-1.79 (quin, *J* = 7.6 Hz, 2H, Ar-O-CH_2-C$\underline{H}_2$-), 1.52-1.26 (m, 20H, -$(CH_2)_{10}$-), 0.88 (t, *J* = 7 Hz, 3H, -CH_3); Elemental analysis: $C_{47}H_{47}NO_7$ requires C 76.51, H 6.41, N 1.89; found C 76.65, H 6.44, N 1.72%.

4-Cyanophenyl-3′-(4-(4-*n*-tetradecyloxybenzoyloxy)benzoyloxy)biphenyl-4-carboxylate, 2.B.5 (X = H)

Yield: (72%); mp 115.5 °C; IR (KBr) ν_{max}: 3103, 3068, 2918, 2848, 2229, 1745, 1733, 1604, 1508, 1473 cm^{-1}; ^{1}H NMR (400 MHz, $CDCl_3$) δ: 8.32 (d, *J* = 8.6 Hz, 2H, Ar-H), 8.27 (d, *J* = 8.6 Hz, 2H, Ar-H), 8.16 (d, *J* = 8.8 Hz, 2H, Ar-H), 7.77 (dd, J_1 = 2.2 Hz, J_2 = 4.1 Hz, 4H, Ar-H), 7.59-7.52 (m, 3H, Ar-H), 7.4 (dd, J_1 = 2 Hz, J_2 = 6.72 Hz, 4H, Ar-H), 7.32-7.28 (m, 1H, Ar-H), 6.99 (d, *J* = 9 Hz, 2H, Ar-H), 4.05 (t, *J* = 6.74 Hz, 2H, Ar-O-CH_2-),1.86-1.79 (quin, *J* = 7.56 Hz, 2H, Ar-O-CH_2-C$\underline{H}_2$-), 1.55-1.26 (m, 22H, -$(CH_2)_{11}$-), 0.88 (t, *J* = 6.64 Hz, 3H, -CH_3); Elemental analysis: $C_{48}H_{49}NO_7$ requires C 76.67, H 6.56, N 1.86; found C 77.12, H 6.86, N 1.49%.

4-Cyanophenyl-3′-(4-(4-*n*-pentadecyloxybenzoyloxy)benzoyloxy)biphenyl-4-carboxylate, 2.B.6 (X = H)

Yield: (75%); mp 116.5 °C; IR (KBr) ν_{max}: 3101, 3070, 2922, 2852, 2235, 1734, 1732, 1602, 1506, 1458, 1377 cm^{-1}; ^{1}H NMR (400 MHz, $CDCl_3$) δ: 8.32 (d, *J* = 8.88 Hz, 2H, Ar-H), 8.27 (d, *J* = 8.88 Hz, 2H, Ar-H), 8.16 (d, *J* = 9.2 Hz, 2H, Ar-H), 7.77 (dd, J_1 = 2 Hz, J_2 = 4.4 Hz, 4H, Ar-H), 7.58-7.52 (m, 3H, Ar-H), 7.39 (dd, J_1 = 2.1 Hz, J_2 = 6.65 Hz, 4H, Ar-H), 7.32-7.28 (m, 1H, Ar-H), 6.99 (d, *J* = 9.2 Hz, 2H, Ar-H), 4.05 (t, *J* = 6.74 Hz, 2H, Ar-O-CH_2-), 1.87-1.79 (quin, *J* = 7.67 Hz, 2H, Ar-O-CH_2-C$\underline{H}_2$-), 1.52-1.26 (m, 24H, -$(CH_2)_{12}$-), 0.88 (t, *J* = 6.6 Hz, 3H, -CH_3); Elemental analysis: $C_{49}H_{51}NO_7$ requires C 76.84, H 6.71, N 1.82; found C 77.11, H 6.93, N 1.86%.

4-Cyanophenyl-3′-(4-(4-*n*-hexadecyloxybenzoyloxy)benzoyloxy)biphenyl-4-carboxylate, 2.B.7 (X = H)

Yield: (73%); mp 115 °C; IR (KBr) ν_{max}: 3093, 3070, 2922, 2852, 2239, 1735, 1732, 1604, 1585, 1506, 1456, 1417 cm^{-1}; ^1H NMR (400 MHz, $CDCl_3$) δ: 8.32 (d, *J* = 8.8 Hz, 2H, Ar-H), 8.27 (d, *J* = 8.88 Hz, 2H, Ar-H), 8.16 (d, *J* = 9 Hz, 2H, Ar-H), 7.77 (dd, J_1 = 2.05 Hz, J_2 = 4.06 Hz, 4H, Ar-H), 7.59-7.53 (m, 3H, Ar-H), 7.39 (dd, J_1 = 2.1 Hz, J_2 = 6.74 Hz, 4H, Ar-H), 7.32-7.28 (m, 1H, Ar-H), 6.99 (d, *J* = 9 Hz, 2H, Ar-H), 4.05 (t, *J* = 6.74 Hz, 2H, Ar-O-CH_2-), 1.86-1.79 (quin, *J* = 7.6 Hz, 2H, Ar-O-CH_2-C$\underline{H}_2$-), 1.52-1.26 (m, 26H, -$(CH_2)_{13}$-), 0.88 (t, *J* = 6.6 Hz, 3H, -CH_3); Elemental analysis: $C_{50}H_{53}NO_7$ requires C 77, H 6.84, N 1.79; found C 76.96, H 7.2, N 1.76%.

4-Cyanophenyl-3′-(4-(4-*n*-octadecyloxybenzoyloxy)benzoyloxy)biphenyl-4-carboxylate, 2.B.8 (X = H)

Yield: (75%); mp 116 °C; IR (KBr) ν_{max}: 3101, 3066, 3049, 2954, 2918, 2850, 2237, 1735, 1732, 1604, 1577, 1508, 1473, 1463 cm^{-1}; ^1H NMR (400 MHz, $CDCl_3$) δ: 8.3 (d, *J* = 8.74 Hz, 2H, Ar-H), 8.25 (d, *J* = 8.5 Hz, 2H, Ar-H), 8.15 (d, *J* = 8.88 Hz, 2H, Ar-H), 7.75 (dd, J_1 = 1.95 Hz, J_2 = 4.45 Hz, 4H, Ar-H), 7.57-7.53 (m, 3H, Ar-H), 7.38 (dd, J_1 = 2.05 Hz, J_2 = 6.73 Hz, 4H, Ar-H), 7.32-7.28 (m, 1H, Ar-H), 6.98 (d, *J* = 8.92 Hz, 2H, Ar-H), 4.04 (t, *J* = 6.54 Hz, 2H, Ar-O-CH_2-), 1.85-1.78 (quin, *J* = 6 Hz, 2H, Ar-O-CH_2-C$\underline{H}_2$-), 1.51-1.19 (m, 30H, -$(CH_2)_{15}$-), 0.86 (t, *J* = 7.01 Hz, 3H, -CH_3); Elemental analysis: $C_{52}H_{57}NO_7$ requires C 77.3, H 7.1, N 1.73; found C 77.04, H 7.49, N 1.64%.

4-Cyanophenyl-3′-(4-(4-*n*-icosyloxybenzoyloxy)benzoyloxy)biphenyl-4-carboxylate, 2.B.9 (X = H)

Yield: (72%); mp 116 °C; IR (KBr) ν_{max}: 3066, 3045, 2954, 2921, 2852, 2239, 1731, 1733, 1604, 1575, 1461, 1454 cm^{-1}; ^1H NMR (400 MHz, $CDCl_3$) δ: 8.3 (d, *J* = 8.76 Hz, 2H, Ar-H), 8.25 (d, *J* = 8.52 Hz, 2H, Ar-H), 8.15 (d, *J* = 8.9 Hz, 2H, Ar-H), 7.76 (dd, J_1 = 2.26 Hz, J_2 = 7.73 Hz, 4H, Ar-H), 7.57-7.52 (m, 3H, Ar-H), 7.39 (dd, J_1 = 2.16 Hz, J_2 = 6.64 Hz, 4H, Ar-H), 7.31-7.28 (m, 1H, Ar-H), 6.99 (d, *J* = 8.96 Hz, 2H, Ar-H), 4.05 (t, *J* = 6.56 Hz, 2H, Ar-O-CH_2-), 1.84-1.79 (quin, *J* = 6.96 Hz, 2H, Ar-O-CH_2-C$\underline{H}_2$-), 1.50-1.21 (m, 34H, -$(CH_2)_{17}$-),

0.87 (t, *J* = 6.68 Hz, 3H, -CH_3); Elemental analysis: $C_{54}H_{61}NO_7$ requires C 77.58, H 7.34, N 1.67; found C 77.73, H 7.17, N 2.02%.

4-Cyano-3-fluorophenyl-3′-(4-(4-*n*-hexadecyloxybenzoyloxy)benzoyloxy)biphenyl-4-carboxylate, 2.B.10 (X = F)

Yield: (70%); mp 114.5 °C; IR (KBr) ν_{max}: 3101, 3073, 2928, 2858, 2235, 1733, 1724, 1604, 1577, 1504, 1473, 1377 cm^{-1}; ^{1}H NMR (400 MHz, $CDCl_3$) δ: 8.31 (d, *J* = 8.6 Hz, 2H, Ar-H), 8.25 (d, *J* = 8.2 Hz, 2H, Ar-H), 8.16 (d, *J* = 8.9 Hz, 2H, Ar-H), 7.78 (d, *J* = 8.4 Hz, 2H, Ar-H), 7.72 (t, *J* = 8.2 Hz, 1H, Ar-H), 7.59-7.53 (m, 4H, Ar-H), 7.4 (d, *J* = 8.2 Hz, 2H, Ar-H), 7.32-7.28 (m, 1H, Ar-H), 7.21 (d, *J* = 8.4 Hz, 1H, Ar-H), 6.99 (d, *J* = 9 Hz, 2H, Ar-H), 4.05 (t, *J* = 6.4 Hz, 2H, Ar-O-CH_2-), 1.82-1.79 (quin, *J* = 7.6 Hz, 2H, Ar-O-CH_2-C$\underline{H}_2$-), 1.52-1.26 (m, 26H, -$(CH_2)_{13}$-), 0.88 (t, *J* = 6.6 Hz, 3H, -CH_3); Elemental analysis: $C_{50}H_{52}FNO_7$ requires C 75.26, H 6.57, N 1.76; found C 75.5, H 6.32, N 1.69%.

4-Cyano-3-fluorophenyl-3′-(4-(4-*n*-octadecyloxybenzoyloxy)benzoyloxy)biphenyl-4-carboxylate, 2.B.11 (X = F)

Yield: (65%); mp 117 ºC; IR (KBr) ν_{max}: 3095, 3070, 2923, 2852, 2235, 1735, 1728, 1608, 1579, 1502, 1461, 1377 cm^{-1}; ^{1}H NMR (400 MHz, $CDCl_3$) δ: 8.31 (d, *J* = 8.69 Hz, 2H, Ar-H), 8.25 (d, *J* = 8.33 Hz, 2H, Ar-H), 8.16 (d, *J* = 8.84 Hz, 2H, Ar-H), 7.78 (d, *J* = 8.39 Hz, 2H, Ar-H), 7.72 (t, *J* = 8.34 Hz, 1H, Ar-H), 7.59-7.53 (m, 4H, Ar-H), 7.4 (d, *J* = 8.68 Hz, 2H, Ar-H), 7.32-7.28 (m, 1H, Ar-H), 7.22 (d, *J* = 8.19 Hz, 1H, Ar-H), 6.99 (d, *J* = 9 Hz, 2H, Ar-H), 4.05 (t, *J* = 6.48 Hz, 2H, Ar-O-CH_2-), 1.84-1.79 (quin, *J* = 6.9 Hz, 2H, Ar-O-CH_2-C$\underline{H}_2$-), 1.51-1.26 (m, 30H, -$(CH_2)_{15}$-), 0.88 (t, *J* = 6.52 Hz, 3H, -CH_3); Elemental analysis: $C_{52}H_{56}FNO_7$ requires C 75.62, H 6.82, N 1.69; found C 75.34, H 6.9, N 1.78%.

4-Cyano-3-fluorophenyl-3′-(4-(4-*n*-icosyloxybenzoyloxy)benzoyloxy)biphenyl-4-carboxylate, 2.B.12 (X = F)

Yield: (68%); mp 118.5 °C; IR (KBr) ν_{max}: 3101, 3070, 2926, 2854, 2237, 1743, 1737, 1604, 1577, 1508, 1473, 1377 cm^{-1}; ^{1}H NMR (400 MHz, $CDCl_3$) δ: 8.31 (d, *J* = 8.64 Hz, 2H, Ar-H), 8.25 (d, *J* = 8.4 Hz, 2H, Ar-H), 8.16 (d, *J* = 8.6 Hz, 2H, Ar-H), 7.78 (d, *J* = 8.3 Hz, 2H, Ar-H), 7.72 (t, *J* = 8.2 Hz, 1H, Ar-H), 7.59-7.54 (m, 4H, Ar-H), 7.4 (d, *J* = 8.3 Hz, 2H, Ar-H),

7.32-7.28 (m, 1H, Ar-H), 7.22 (d, *J* = 8.2 Hz, 1H, Ar-H), 6.99 (d, *J* = 9.1 Hz, 2H, Ar-H), 4.05 (t, *J* = 6.42 Hz, 2H, Ar-O-CH_2-), 1.83-1.79 (quin, *J* = 7 Hz, 2H, Ar-O-CH_2-C$\underline{H}_2$-), 1.51-1.26 (m, 34H, -$(CH_2)_{17}$-), 0.88 (t, *J* = 6.58 Hz, 3H, -CH_3); Elemental analysis: $C_{54}H_{60}FNO_7$ requires C 75.94, H 7.08, N 1.64; found C 75.74, H 7.2, N 1.77%.

References

[1] Niori, T.; Sekine, T.; Watanabe, J.; Furukawa, T.; Takezoe, H. *J. Mater. Chem.* **1996**, *6*, 1231-1233.

[2] Link, D. R.; Natale, G.; Shao, R.; Maclennan, J. E.; Clark, N. A.; Korblova, E.; Walba, D. M. *Science* **1997**, *278*, 1924-1927.

[3] Pelzl, G.; Diele, S.; Weissflog, W. *Adv. Mater.* **1999**, *11*, 707-724.

[4] Reddy, R. A.; Tschierske, C. *J. Mater. Chem.* **2006**, *16*, 907-961.

[5] Takezoe, H.; Takanishi, Y. *Jpn. J. Appl. Phys.* **2006**, *45*, 597-625.

[6] de Gennes, P. G. *The Physics of Liquid Crystals;* Clarendon Press: Oxford, 1974, p 279.

[7] Brand, H. R.; Cladis, P. E.; Pleiner, H. *Macromolecules* **1992,** *25*, 7223-7226.

[8] Leube, H. F.; Finkelmann, H. *Makromol. Chem.* **1991**, *192*, 1317-1328.

[9] Pratibha, R.; Madhusudana, N. V.; Sadashiva, B. K. *Science* **2000**, *288*, 2184-2187.

[10] Hegmann, T.; Kain, J.; Diele, S.; Pelzl, G.; Tschierske, C. *Angew. Chem. Int. Ed.* **2001**, *40*, 887-890.

[11] Semmler, H. J. K.; Dingemans, T. J.; Samulski, E. T. *Liq. Cryst.* **1998,** *24***,** 799-803.

[12] Eremin, A.; Diele, S.; Pelzl, G.; Nadasi, H.; Weissflog, W.; Salfetnikova, J.; Kresse, H. *Phy. Rev. E* **2001**, *64*, 051707.

[13] Sadashiva, B. K.; Reddy, R. A.; Pratibha, R.; Madhusudana, N. V. *Chem. Commun.* **2001**, 2140-2141.

[14] Sadashiva, B. K.; Reddy, R. A.; Pratibha, R.; Madhusudana, N. V. *J. Mater. Chem.* **2002**, *12*, 943-950.

[15] Reddy, R. A.; Sadashiva, B. K. *J. Mater. Chem.* **2004**, *14*, 310-319.

[16] Murthy, H. N. S.; Sadashiva, B. K. *Liq. Cryst.* **2004**, *31*, 567-578.

[17] Mieczkowski, J.; Gomola, K.; Koseska, J.; Pociecha, D.; Szydlowska, J.; Gorecka, E. *J. Mater. Chem.* **2003**, *13*, 2132-2137.

[18] Pociecha, D.; Čepič, M.; Gorecka, E.; Mieczkowski, J. *Phys. Rev. Lett.* **2003**, *91*, 185501.

[19] Shimbo, Y.; Gorecka, E.; Pociecha, D.; Aroaka, F.; Goto, M.; Takanishi, Y.; Ishikawa, K.; Mieczkowski, J.; Gomola, K.; Takezoe, H. *Phys. Rev. Lett.* **2006**, *97*, 113901.

[20] Shimbo, Y.; Takanishi, Y.; Ishikawa, K.; Gorecka, E.; Pociecha, D.; Mieczkowski, J.; Gomola, K.; Takezoe, H. *Jpn. J. Appl. Phys.* **2006**, *45*, L282-L284.

[21] Gomola, K.; Guo, L.; Dhara, S.; Shimbo, E.; Gorecka, E.; Pociecha, D.; Mieczkowski, J.; Takezoe, H. *J. Mater. Chem.* **2009**, *19*, 4240-4247.

[22] Gomola, K.; Guo, L.; Gorecka, E.; Pociecha, D.; Mieczkowski, J.; Ishikawa, K.; Takezoe, H. *Chem. Commun.* **2009,** 6592-6594.

[23] Guo, L.; Gomola, K.; Gorecka, E.; Pociecha, D.; Dhara, S.; Araoka, F.; Ishikawa, K.; Takezoe, H. *Soft Matter* **2010**, *7*, 2895-2899.

[24] Keith, C.; Prehm, M.; Panarin, Y. P.; Vij, J. K.; Tschierske, C. *Chem. Commun.* **2010,** *46*, 3702-3704.

[25] Reddy, R. A.; Zhu, C. Z.; Shao, R.; Korblova, E.; Gong, T.; Shen, Y.; Garcia, E.; Glaser, M. A.; Maclennan, J. E.; Walba, D. M.; Clark, N. A. *Science* **2011**, *332*, 72-77.

[26] Guo, L.; Dhara, S.; Sadashiva, B. K.; Radhika, S.; Pratibha, R.; Shimbo, Y.; Araoka, F.; Ishikawa, K.; Takezoe, H. *Phy. Rev. E* **2010**, *81*, 011703.

[27] Gupta, M.; Datta, S.; Radhika, S.; Sadashiva, B. K.; Roy, A. *Soft Matter* **2011**, *7*, 4735-4741.

[28] Miyasato, K.; Abe, S.; Takezoe, H.; Fukuda, A.; Kuze, E. *Jpn. J. Appl. Phys.* **1983,** *22*, L661- L663.

[29] Gray, G. W.; Jones, B. *J. Chem. Soc.* **1953,** 4179-4180.

[30] Murthy, H. N. S.; Sadashiva, B. K. *J. Mater. Chem.* **2004,** *14*, 2813-2821.